Figure 1. MD simulation of the identical gp120 outer domain carrying a V3 loop with net charge of +7 or +3. (A) Schematic representation of the gp120 open reading frame along with the amino acid sequences. The net charge indicates the number of positively charged amino acids (R, K, and H) minus the number of negatively charged amino acids (D and E) in the V3 loop. A light blue box indicates the outer domain used for the MD simulations. A pink box indicates the V3 loop. The numbers indicate amino acid positions at the outer domain (amino acids 1 to 233 in Figure 1A correspond to amino acids 256 to 489 in the gp120 of HIV-1_{LAI}) or the V3 loop. An open black box in the V3 loop sequence indicates a potential site for the N-linked glycosylation. (B–D) Left panels: $Gp120_{LAI\text{-}NH1V3}$; Right panels: $Gp120_{LAI\text{-}TH09V3}$. +7 and +3 indicate the net charges of V3 loops of the recombinant proteins. (B) Time course of RMSD during MD simulations. The RMSD values indicate the structural fluctuations of the outer domain in aqueous solution. The numbers in the horizontal axes indicate the time of MD simulation. (C) Distribution of RMSF in the gp120 outer domain. The RMSF values indicate the atomic fluctuations of the main chains of individual amino acids during 10–30 ns of MD simulations. The numbers in the horizontal axes indicate amino acid positions at the outer domain. (D) Superimposition of Gp120 models at 10, 15, 20, 25, and 30 ns of MD simulation. A green asterisk indicates approximate position of a potential N-glycosylation site at the V3 stem. A green arrow indicates the site of the disulfide bond at the V3 base.
doi:10.1371/journal.pone.0037530.g001

previous [12,13,14,15,16] neutralization studies raised the possibility that the gp120 surface might be less heterogeneous in gp120 subpopulations that have a less positively charged V3 loop, due to greater magnitudes of resistance to the antibody neutralization. To address this possibility, we performed an information entropy study using sequences in the public database. We extracted full-length gp120 amino acid sequences of HIV-1 subtype CRF01_AE that has the same evolutionary origin and is spread throughout southeast Asia [42]), and divided them into subgroups on the basis of the net charge of V3 loop (+2, +3, +4, +5, +6, +7, and +8). The sequences were used to calculate the Shannon entropy scores, *H(i)* [1], to denote the diversity of individual amino acids within each subpopulation.

Figure 3 shows the 3-D distribution of the *H(i)* scores of individual amino acids plotted on the HIV-1 gp120 crystal structure (PDB code: 2B4C [1]), where the green to orange regions were suggested to have more variable amino acids than the blue ones. In the gp120 subpopulation that has +7 V3 loop, the *H(i)* scores often exceeded 2.0 bits at many residues, reaching close to the maximum value of 4.4, i.e., the diversity was maximal, at the V5 region (Fig. 3A, left panel). Regions with high *H(i)* scores included the functional sites, such as the V3 loop and the regions around the CD4 binding site. In marked contrast, in the gp120 subpopulation carrying the +3 V3 loop, the *H(i)* scores were almost zero, i.e., the diversity was minimal, at many amino acids, but not at those in the V4, V5, and *L*E regions (Fig. 3A, right panel). Importantly, relatively high levels of conservation were also detected with amino acids in the otherwise highly variable V3 loop. Moreover, a region adjacent to the CD4 binding loop was also less heterogeneous compared with those of the gp120 subpopulation carrying +7 V3 loop (Figs. 3B). In the gp120 subpopulations carrying the +2, +3, 4, and +5 V3 loops, the *H(i)* scores were indistinguishable from each other: they were less heterogeneous than the subpopulations carrying the +6, +7, and +8 V3 loops. Similar results were obtained with HIV-1 subtype C that represents the most predominated HIV-1 in the world (data not shown).

Discussion

The ability of HIV-1 to rapidly change its phenotype greatly complicates our efforts to eradicate this virus. Elucidation of structural principles for the phenotypic change may provide a clue to control HIV-1. In this study, by combining MD simulations with antibody neutralization experiments and diversity analysis of the viral protein sequences, we studied a structural basis for the phenotypic change of HIV-1 by V3 mutations. To address this issue, we used a V3 recombinant system; we performed a computer-assisted structural study and an infection-based neutralization assay using gp120 proteins whose amino acid sequences are identical except for V3 loop. In combination with an informatics study, we obtained evidence that the HIV-1 V3 loop acts as an electrostatic modulator that influences the global structure and diversity of the interaction surface of the gp120 outer domain.

Using MD simulation, we first examined whether the V3 net charge could affect the structural dynamics of the HIV-1 gp120 outer domain surface. Initial structures of the outer domain of the two gp120s, $Gp120_{LAI\text{-}NH1V3}$ and $Gp120_{LAI\text{-}TH09V3}$, were identical before MD simulations, because the domains were both derived from HIV-1_{LAI} strain. Remarkably, however, the two molecules with distinct V3 loop exhibited markedly distinct structural dynamics following MD simulations (Figs. 1 and 2). These data strongly suggest that the V3 net charge can act as an intrinsic modulator that influences the structural dynamics of the interaction surface of the gp120 outer domain. Such a global effect on structure by a local electrostatic change has been reported with bacteriorhodopsin [43]. In general, the long-range effects of non-electrostatic contributions are negligible, whereas those of the electrostatic contributions are not [34]. Therefore, it is reasonable that the changes in overall charge of the V3 loop element caused the global effects on the gp120 structure via alteration of the electrostatic potentials of the gp120 surface.

We next studied biological impact of the structural changes predicted by MD simulations. The MD simulations suggested that the CD4 binding loop was less exposed in the $Gp120_{LAI\text{-}NH1V3}$ than the $Gp120_{LAI\text{-}NH1V3}$ (Fig. 2). The finding predicted that reduction in V3 net charge could cause reduction in neutralization sensitivity to the anti-CD4 binding site antibodies. This possibility was assessed by neutralization assay. We used infectious HIV-1_{LAI} clones having the $Gp120_{LAI\text{-}NH1V3}$ or the $Gp120_{LAI\text{-}TH09V3}$ to assess their neutralization sensitivities to the anti-CD4 binding site MAbs. Notably, we indeed observed marked reduction in the neutralization sensitivity in HIV-1_{LAI} having $Gp120_{LAI\text{-}TH09V3}$ (Table 1). The results are consistent with the structural changes predicted by MD simulations, as well as previous findings on neutralization sensitivity of HIV-1s to soluble CD4 [14,15,16].

We further studied evolutionary impact predicted by MD simulations and the neutralization studies. These studies predicted that reduction in V3 net charge could cause reduction in sequence diversity around the CD4 binding site due to reduced sensitivity to positive selection pressures of antibodies. Notably, we indeed observed marked reduction in the gp120 diversity: our Shannon entropy data show that otherwise variable surfaces of gp120, such as V3 and a region around the CD4 binding loop, are less heterogeneous in the gp120 subgroups carrying a V3 loop with a +3 charge (Fig. 3).

Previous cryo-electron microscopy studies have indicated that gp120 forms a trimer on an HIV-1 virion, where the CD4 binding sites are exposed on the outside surface in the solution [44,45,46]. Therefore, it is reasonable that gp120 with +3 V3 with less exposed CD4 binding loop is less sensitive to neutralization by anti-CD4 binding site antibodies (Table 1) and less heterogeneous around the CD4 binding site (Fig. 3). Collectively, our results

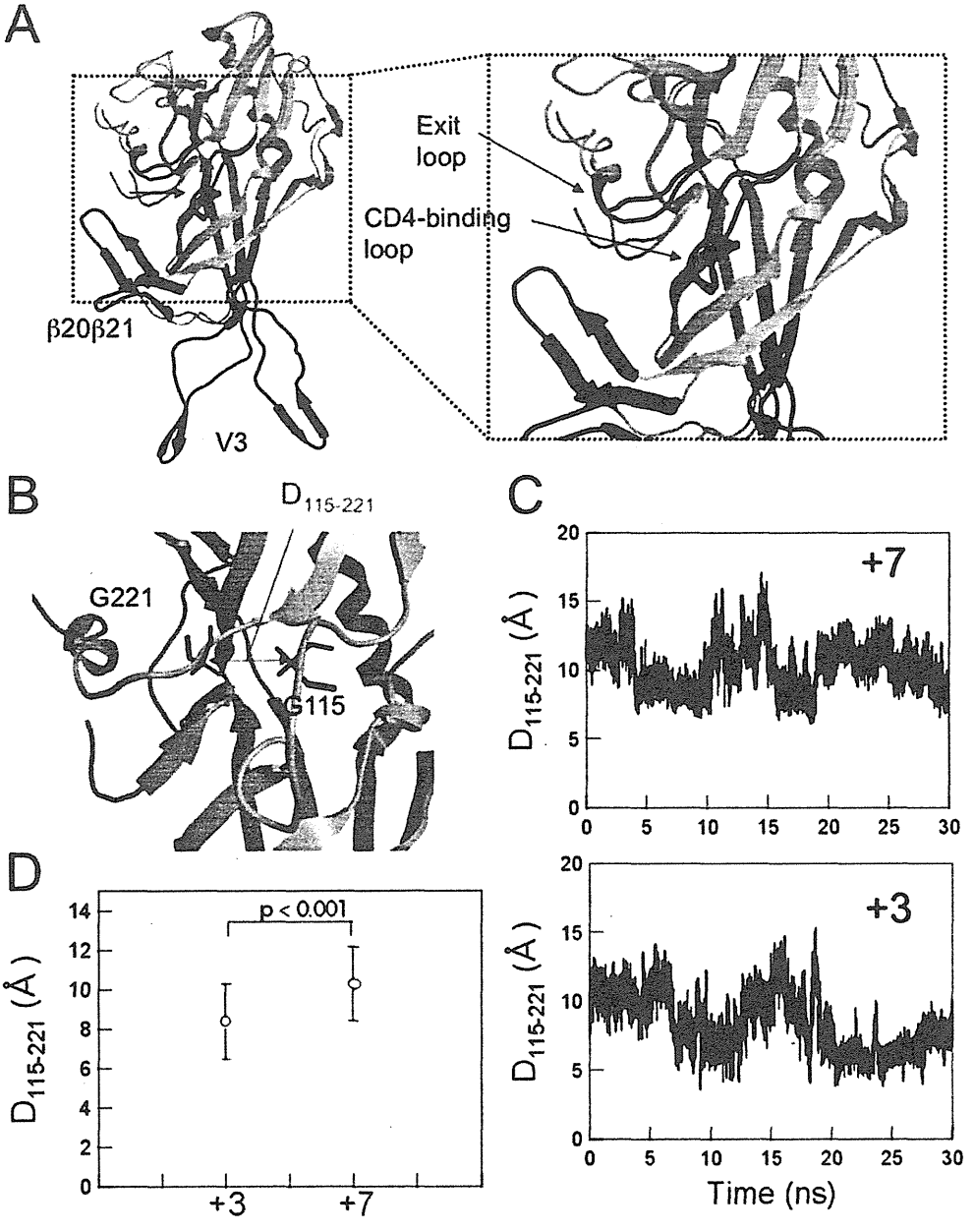

Figure 2. Comparison of the averaged 3-D models during MD simulation. (A) Superposition of the averaged structures obtained with the 40,000 snapshots obtained from 10–30 ns of MD simulations using ptraj module in Amber 9. Red and Blue ribbons: loops of $Gp120_{LAI\text{-}NH1V3}$ and $Gp120_{LAI\text{-}TH09V3}$ with V3 net charges of +7 and +3, respectively. (B–D) Configuration and structural dynamics of the CD4 binding loop. The distance between the Cα of Gly115 and the Cα of Gly221 in the CD4 binding loop was calculated to monitor configurational changes (B). The distance was monitored during the 10–30 ns of MD simulation (C) and the average distance with variance was plotted (D). +7: $Gp120_{LAI\text{-}NH1V3}$; +3: $Gp120_{LAI\text{-}TH09V3}$.
doi:10.1371/journal.pone.0037530.g002

obtained with all three approaches agree with each other and suggest that V3 net charge is an intrinsic factor that influences structural property, antibody sensitivity, and sequence diversity of CD4 binding site.

The HIV-1 gp120 outer domain has several functional or immunogenic loops involved in binding to CD4, coreceptor and antibodies. Our MD simulations predicted that V3 net charge influences fluctuation and conformation of these loops (Figs. 1 and 2). The V3-based structural modulation of the gp120 surface loops may be an effective mechanism to alter effectively the phenotype and relative fitness of HIV-1. For example, a change in the V3 net charge by mutations may induce changes in V3 conformation (Figs. 1D and 2A) [13], which in turn may influence intra- or inter-molecular interactions among gp120 monomers and thus global structure of gp120 trimer on a virion. Generation of a swarm of structural variants by V3 mutations could help generating the best-

Table 1. Neutralization sensitivity of the isogenic V3 recombinant HIV-1 to anti-gp120 monoclonal antibodies.

Antibody ID	Ig subtype	Epitopes on Gp120	ND_{50} (μg/ml)[@]	
			$HIV\text{-}1_{LAI\text{-}NH1V3}$	$HIV\text{-}1_{LAI\text{-}TH09V3}$
49G2	human IgG1	CD4 binding site[#]	0.224	>10
42F9	human IgG1	CD4 binding site[#]	0.934	>10
0.5δ [59]	human IgG1	CD4 binding site[#]	0.444	>10
4C11 [59]	human IgG2	CD4 induced structure[$]	>20	>10
4301	mouse IgG	broadly reactive*	0.59	0.57
8D11	human IgG1	none	>20	>10

[#]Neutralization epitope in the Gp120 outer domain before CD4 binding.
[$]Neutralization epitope induced in Gp120 after CD4 binding.
*Epitopes outside of the CD4 binding site [37].
[@]The effect of each antibody on viral infectivity was tested in duplicate.
doi:10.1371/journal.pone.0037530.t001

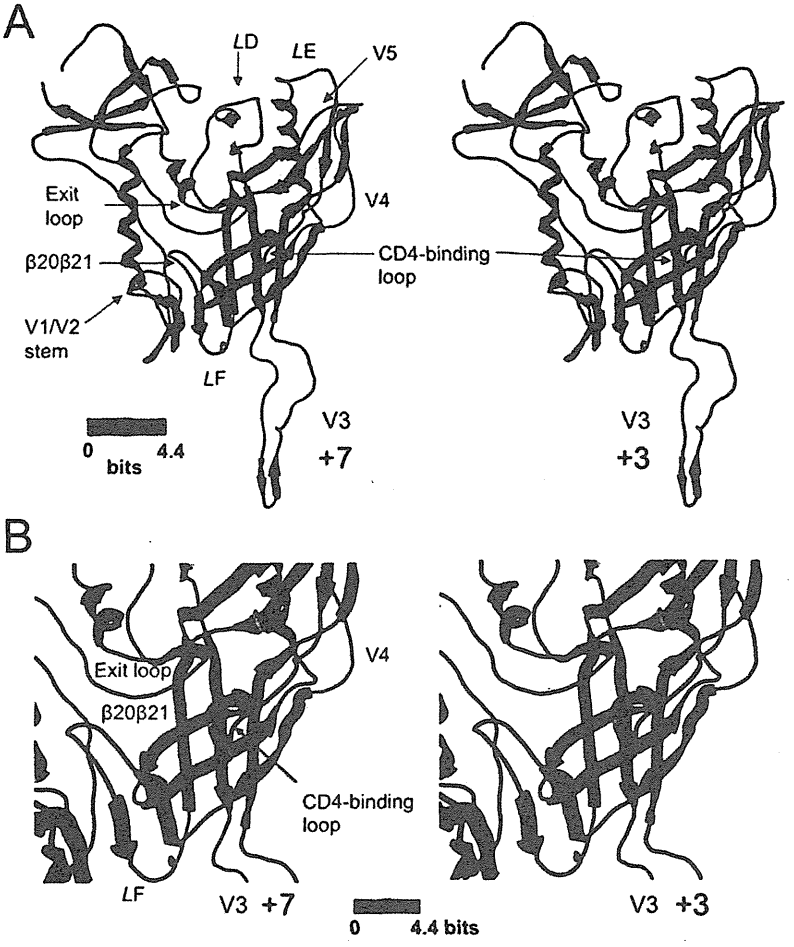

Figure 3. Diversity of the gp120 subpopulations carrying a V3 loop with net charge of +7 or +3. Full-length gp120 sequences of the HIV-1 CRF01_AE [42] were extracted from a public database, and divided into subgroups on the basis of the net charge of the V3 loop (+2~+8). The divided sequences were used to calculate the Shannon entropy, *H(i)* [63], within each subpopulation, and the *H(i)* values were plotted on the 3-D structure of gp120 (PDB code: 2B4C [1]). The results for the gp120 subgroups that have V3 loops with +7 (left panel) and +3 (right panel) charges are shown as representative. The numbers of sequences used to calculate the *H(i)* were 9 and 81 for +7 and +3, respectively. (A) Distribution of *H(i)* in the gp120 monomer. (B) Distribution of *H(i)* around the CD4 binding site.
doi:10.1371/journal.pone.0037530.g003

fit variants under changing environments during persistent infection of HIV-1 *in vivo*. Further study is necessary to address above issue.

Thus far fine structures of neither the intact gp120 monomer nor trimer are available. However, recent crystal structure study disclosed a structure of V1/V2 domain [47], which had been the major gp120 region lacking structural information. The V1/V2 domain is located on the outer surface of gp120, as is V3, and can participate in phenotypic changes of HIV-1 [48,49]. In this regard, Kwon et al [50] have found an intriguing role of gp120 variable loops; gp120 core has an intrinsic preference to form the CD4-bound conformation, whereas the variable loops, such as V1/V2 and V3 loops, play key roles in preventing conformational transitions into the CD4-bound state that is sensitive to neutralization. Thus it is conceivable that configurational changes of V3 loop by V3 mutations play roles in modulating structural dynamics of the unliganded gp120 core and neutralization sensitivity of HIV-1. Availability of the V1/V2 loop structure will promote structural study of the whole gp120 monomer containing V3 loop, V1/V2 domain, and glycans. Our findings will provide a structural basis to elucidate intra-molecular interactions of these elements, which in turn will allow the study of structure, function, and evolution of gp120 trimer. Incorporation of MD simulation into these studies will help understanding structural dynamics with which HIV-1 adjusts its relative replication fitness in nature.

Materials and Methods

Characteristics of the gp120 proteins and HIV-1s used

We used two isogenic recombinant gp120 proteins, termed $Gp120_{LAI\text{-}NH1V3}$ and $Gp120_{LAI\text{-}TH09V3}$ [35], for the present structural and neutralization studies. They differ only in their V3 loops. The $Gp120_{LAI\text{-}NH1V3}$ and $Gp120_{LAI\text{-}TH09V3}$ have the 35-amino-acid-length V3 loops from HIV-1-infected individuals in the gp120 backbone of the HIV-1_{LAI} strain [35]. The net charges of the V3 loops are +7 and +3 for the $Gp120_{LAI\text{-}NH1V3}$ and $Gp120_{LAI\text{-}TH09V3}$, respectively (the V3 net charge represents the number of positively charged amino acids (R, K, and H) minus the number of negatively charged amino acids (D and E) in the V3 loop). The HIV-1_{LAI} carrying the $Gp120_{LAI\text{-}NH1V3}$ (HIV-$1_{LAI\text{-}NH1V3}$) is the CXCR4 tropic virus, whereas that carrying the $Gp120_{LAI\text{-}TH09V3}$ (HIV-$1_{LAI\text{-}TH09V3}$) is the CCR5 monotropic virus [35]. The HIV-$1_{LAI\text{-}NH1V3}$ is sensitive to neutralization by antibodies with the ability to bind to the peptides containing the autologous V3 tip sequences, whereas HIV-$1_{LAI\text{-}TH09V3}$ is highly resistant to antibodies targeting the autologous V3 tip sequences [13].

MD simulation

As the initial structures for the MD simulation, we first constructed three-dimensional (3-D) models of the outer domains of the $Gp120_{LAI\text{-}NH1V3}$ and $Gp120_{LAI\text{-}TH09V3}$ by the comparative (homology) modeling method (reviewed in [33,51,52]), as described previously [13]. We used the crystal structure of HIV-1 gp120 containing an entire V3 region at a resolution of 3.30 Å (PDB code: 2B4C [1]) as the modeling template. The gp120 core is in complex with the CD4 receptor and the CD4 induced structure (CD4i) antibody X5 [1]: it represents the structure after the CD4 binding. We deleted the structures of the CD4 receptor and the X5 antibody from the 2B4C complex structure to construct the free gp120 outer domain models of HIV-1_{LAI} V3 recombinant viruses by homology modeling. Then the models were subjected to the MD simulations to analyze structure and dynamics of the gp120 outer domain in the absence of the CD4 receptor and the X5 antibody interactions. The homology modeling was performed using tools available in the Molecular Operating Environment (MOE) program (MOE 2008.10; Chemical Computing Group Inc., Montreal, Quebec, Canada). The 186 amino-terminal and 27 carboxyl-terminal residues were deleted to construct the gp120 outer domain structure. We optimized the 3-D structure thermodynamically via energy minimization using an MOE and an AMBER99 force field [53]. We further refined the physically unacceptable local structure of the models based on a Ramachandran plot evaluation using MOE. MD simulations were performed as described previously [13] using the Sander module in the Amber 9 program package [54] and the AMBER99SB force field [55] with the TIP3P water model [56]. Bond lengths involving hydrogen were constrained with the SHAKE algorithm [57], and the time step for all MD simulations was set to 2 fs. A nonbonded cutoff of 12 Å was used. After heating calculations for 20 ps to 310 K using the NVT ensemble, the simulations were executed using the NPT ensemble at 1 atm at 310 K for 30 ns. Superimpositions of the $Gp120_{LAI\text{-}NH1V3}$ and $Gp120_{LAI\text{-}TH09V3}$ structures were done by coordinating atoms of amino acids along the β-sheet at the gp120 outer domain. We performed two independent MD simulations with distinct MD codes and obtained similar results. Therefore, we present here the data set from one of the MD simulations as a representation.

Calculation of the root mean square deviation (RMSD) and root mean square fluctuation (RMSF)

The RMSD values between the heavy atoms of the two superposed proteins were used to measure the overall structural differences between the two proteins [34]. We also calculated the RMSF to provide information about the atomic fluctuations during MD simulations [34]. In this study, we calculated the RMSF of the main chains of individual amino acids using the 40,000 snapshots obtained from MD simulations of 10–30 ns. The average structures during the last 20 ns of MD simulations were used as reference structures for the calculation of the RMSF. Both the RMSD and RMSF were calculated using the ptraj module in Amber 9 [34].

Monoclonal antibodies (MAbs)

The 49G2, 42F9, 0.5δ and 4C11 antibodies used for the neutralization assay were the human MAbs established from an HIV-1-infected patient with long-term non-progressive illness. Human blood samples were collected after signed informed consent in accordance with study protocol and informed consent reviewed and approved by Ethics committee for clinical research & advanced medical technology at the Faculty of Life Science Kumamoto University. B cells from the patient's peripheral blood mononuclear cells were transformed by EBV, followed by cloning as described previously [58]. The culture supernatant from an individual clone was screened for the reactivity to $gp120_{SF2}$ by an enzyme-linked immunosorbent assay (ELISA). The specificity of antibodies was determined by gp120 capture ELISA and FACS analysis as described previously [59]. Briefly, reactivity of the mAbs against monomeric gp120 of HIV-1_{SF2} was measured with a gp120 capture assay in the absence or presence of soluble CD4 (0.5 μg/ml). Decrease in the binding activity was observed for the mAbs 0.5δ, 49G2, and 42F9 in the presence of soluble CD4, whereas enhancement in the reactivity was detected for the mAb 4C11. Reactivity of the mAbs against envelope protein on the cell surface was measured with a FACS analysis of PM1 cells chronically infected with JR-FL in the absence or presence of soluble CD4 (0.5 μg/ml). No significant difference was observed for the binding profiles of 0.5δ, 49G2, and 42F9 in the presence of

soluble CD4, whereas marked enhancement of binding was observed for the 4C11 in the presence of soluble CD4. Based on these binding data, we classified 49G2, 42F9, and 0.5δ as CD4 binding site Mabs, and 4C11 as a CD4-induced epitope. All MAbs used in this study were purified by affinity chromatography on Protein A Sepharose. A human MAb 8D11 was used as a negative control for the neutralization assay. Mouse MAb 4301 was purchased from Advanced BioScience Laboratories, Inc. (Kensington, MD). The 4301 was raised with a mixture of purified gp120 of HIV-1_{IIIB} and HIV-1_{MN} and broadly reactive with the gp120 of different HIV-1 isolates [37].

Neutralization assay

We used the two above-described V3 recombinant HIV-1s, HIV-$1_{LAI\text{-}NH1V3}$ and HIV-$1_{LAI\text{-}TH09V3}$ [35], for the neutralization study. The HIV-1 cell-free viruses were prepared by transfection of the plasmid DNAs into HeLa cells as described previously [24,35,60]. The neutralization activities of antibodies were measured in a single-round viral infectivity assay using $CD4^+CXCR4^+CCR5^+$ HeLa cells [36] as described previously [13]. Briefly, equal infectious titers of viruses (300 blue-cell-forming units) were incubated with serially diluted MAb preparations (0.03–10 μg/ml) for 1 hour at 37°C. The cells were infected with the virus-antibody mixture for 48 hours at 37°C, fixed, and stained with 5-bromo-4-chloro-3-indolyl-β-D-galactopyranoside. Each antibody dilution was tested in duplicate, and the means of the positive blue cell numbers were used to calculate the 50% inhibition dose of viral infectivity (ND_{50}).

Analysis of amino acid diversity

Amino acid diversity at individual sites of the HIV-1 gp120 sequences was analyzed with Shannon entropy scores as described previously [13,61,62]. Full-length gp120 amino acid sequences of the HIV-1 subtypes CRF01_AE and C were obtained from the HIV Sequence Database (http://www.hiv.lanl.gov/content/sequence/HIV/mainpage.html). The sequences were divided into subgroups based on the net charge of V3 loop (+2~+8) using a software system, InforSense 5.0.1 (InforSense Ltd. http://www.inforsense.com/); arginine (R), lysine (K), and histidine (H) were counted as +1, aspartic acid (D) and glutamic acid (E) as -1, and other amino acids as 0. The numbers of sequences used for the analysis of CRF01_AE were 11, 81, 57, 28, 18, 9, and 4 for +2, +3, +4, +5, +6, +7, and +8, respectively. The amino acid diversity within each V3 subpopulation of the same HIV-1 subtype was calculated using Shannon's formula [63]:

$$H(i) = -\sum_{x_i} p(x_i)\log_2 p(x_i) \quad \{x_i = \text{G, A, I, V, ...}\},$$

where $H(i)$, $p(x_i)$, and i indicate the amino acid entropy score of a given position, the probability of occurrence of a given amino acid at the position, and the number of the position, respectively. An $H(i)$ score of zero indicates absolute conservation, whereas 4.4 bits indicates complete randomness. The $H(i)$ scores were displayed on the 3-D structure of an HIV-1 gp120 (PDB code: 2B4C [1]).

Acknowledgments

We thank Shingo Kiyoura (SGI Japan, Ltd.), and Kaori Sawada and Takashi Ikegami (Ryoka Systems Inc.) for their support with the computational analysis. We thank Hirotaka Ode of the Pathogen Genomics Center for his helpful comments on the manuscript.

Author Contributions

Conceived and designed the experiments: MY SN HS. Performed the experiments: MY SN HS. Analyzed the data: MY SN HS. Contributed reagents/materials/analysis tools: KY SM. Wrote the paper: MY HS.

References

1. Huang CC, Tang M, Zhang MY, Majeed S, Montabana E, et al. (2005) Structure of a V3-containing HIV-1 gp120 core. Science 310: 1025–1028.
2. Huang CC, Lam SN, Acharya P, Tang M, Xiang SH, et al. (2007) Structures of the CCR5 N terminus and of a tyrosine-sulfated antibody with HIV-1 gp120 and CD4. Science 317: 1930–1934.
3. Choe H, Farzan M, Sun Y, Sullivan N, Rollins B, et al. (1996) The beta-chemokine receptors CCR3 and CCR5 facilitate infection by primary HIV-1 isolates. Cell 85: 1135–1148.
4. Speck RF, Wehrly K, Platt EJ, Atchison RE, Charo IF, et al. (1997) Selective employment of chemokine receptors as human immunodeficiency virus type 1 coreceptors determined by individual amino acids within the envelope V3 loop. J Virol 71: 7136–7139.
5. Xiao L, Owen SM, Goldman I, Lal AA, deJong JJ, et al. (1998) CCR5 coreceptor usage of non-syncytium-inducing primary HIV-1 is independent of phylogenetically distinct global HIV-1 isolates: delineation of consensus motif in the V3 domain that predicts CCR-5 usage. Virology 240: 83–92.
6. Cho MW, Lee MK, Carney MC, Berson JF, Doms RW, et al. (1998) Identification of determinants on a dualtropic human immunodeficiency virus type 1 envelope glycoprotein that confer usage of CXCR4. J Virol 72: 2509–2515.
7. Goudsmit J, Debouck C, Meloen RH, Smit L, Bakker M, et al. (1988) Human immunodeficiency virus type 1 neutralization epitope with conserved architecture elicits early type-specific antibodies in experimentally infected chimpanzees. Proc Natl Acad Sci U S A 85: 4478–4482.
8. Rusche JR, Javaherian K, McDanal C, Petro J, Lynn DL, et al. (1988) Antibodies that inhibit fusion of human immunodeficiency virus-infected cells bind a 24-amino acid sequence of the viral envelope, gp120. Proc Natl Acad Sci U S A 85: 3198–3202.
9. Javaherian K, Langlois AJ, McDanal C, Ross KL, Eckler LI, et al. (1989) Principal neutralizing domain of the human immunodeficiency virus type 1 envelope protein. Proc Natl Acad Sci U S A 86: 6768–6772.
10. Cavacini LA, Duval M, Robinson J, Posner MR (2002) Interactions of human antibodies, epitope exposure, antibody binding and neutralization of primary isolate HIV-1 virions. Aids 16: 2409–2417.
11. Lusso P, Earl PL, Sironi F, Santoro F, Ripamonti C, et al. (2005) Cryptic nature of a conserved, CD4-inducible V3 loop neutralization epitope in the native envelope glycoprotein oligomer of CCR5-restricted, but not CXCR4-using, primary human immunodeficiency virus type 1 strains. J Virol 79: 6957–6968.
12. Bou-Habib DC, Roderiquez G, Oravecz T, Berman PW, Lusso P, et al. (1994) Cryptic nature of envelope V3 region epitopes protects primary monocytotropic human immunodeficiency virus type 1 from antibody neutralization. J Virol 68: 6006–6013.
13. Naganawa S, Yokoyama M, Shiino T, Suzuki T, Ishigatsubo Y, et al. (2008) Net positive charge of HIV-1 CRF01_AE V3 sequence regulates viral sensitivity to humoral immunity. PLoS One 3: e3206.
14. Hwang SS, Boyle TJ, Lyerly HK, Cullen BR (1992) Identification of envelope V3 loop as the major determinant of CD4 neutralization sensitivity of HIV-1. Science 257: 535–537.
15. Willey RL, Theodore TS, Martin MA (1994) Amino acid substitutions in the human immunodeficiency virus type 1 gp120 V3 loop that change viral tropism also alter physical and functional properties of the virion envelope. J Virol 68: 4409–4419.
16. Willey RL, Martin MA, Peden KW (1994) Increase in soluble CD4 binding to and CD4-induced dissociation of gp120 from virions correlates with infectivity of human immunodeficiency virus type 1. J Virol 68: 1029–1039.
17. Kwong PD, Wyatt R, Robinson J, Sweet RW, Sodroski J, et al. (1998) Structure of an HIV gp120 envelope glycoprotein in complex with the CD4 receptor and a neutralizing human antibody. Nature 393: 648–659.
18. Fouchier RA, Groenink M, Kootstra NA, Tersmette M, Huisman HG, et al. (1992) Phenotype-associated sequence variation in the third variable domain of the human immunodeficiency virus type 1 gp120 molecule. J Virol 66: 3183–3187.
19. Chesebro B, Wehrly K, Nishio J, Perryman S (1992) Macrophage-tropic human immunodeficiency virus isolates from different patients exhibit unusual V3 envelope sequence homogeneity in comparison with T-cell-tropic isolates: definition of critical amino acids involved in cell tropism. J Virol 66: 6547–6554.
20. Milich L, Margolin B, Swanstrom R (1993) V3 loop of the human immunodeficiency virus type 1 Env protein: interpreting sequence variability. J Virol 67: 5623–5634.
21. Milich L, Margolin BH, Swanstrom R (1997) Patterns of amino acid variability in NSI-like and SI-like V3 sequences and a linked change in the CD4-binding domain of the HIV-1 Env protein. Virology 239: 108–118.

22. de Jong J-J, de Ronde A, Keulen W, Tersmette M, Goudsmit J (1992) Minimal requirements for the human immunodeficiency virus type 1 V3 domain to support the syncytium-inducing phenotype: analysis by single amino acid substitution. J Virol 66: 6777–6780.
23. Shioda T, Oka S, Ida S, Nokihara K, Toriyoshi H, et al. (1994) A naturally occurring single basic amino acid substitution in the V3 region of the human immunodeficiency virus type 1 env protein alters the cellular host range and antigenic structure of the virus. J Virol 68: 7689–7696.
24. Kato K, Sato H, Takebe Y (1999) Role of naturally occurring basic amino acid substitutions in the human immunodeficiency virus type 1 subtype E envelope V3 loop on viral coreceptor usage and cell tropism. J Virol 73: 5320–5326.
25. Thorpe IF, Brooks CL, 3rd (2007) Molecular evolution of affinity and flexibility in the immune system. Proc Natl Acad Sci U S A 104: 8821–8826.
26. Lu HP, Xun L, Xie XS (1998) Single-molecule enzymatic dynamics. Science 282: 1877–1882.
27. Astumian RD (1997) Thermodynamics and kinetics of a Brownian motor. Science 276: 917–922.
28. Garcia-Viloca M, Gao J, Karplus M, Truhlar DG (2004) How enzymes work: analysis by modern rate theory and computer simulations. Science 303: 186–195.
29. Karplus M, Kuriyan J (2005) Molecular dynamics and protein function. Proc Natl Acad Sci U S A 102: 6679–6685.
30. Dodson GG, Lane DP, Verma CS (2008) Molecular simulations of protein dynamics: new windows on mechanisms in biology. EMBO Rep 9: 144–150.
31. Miyamoto T, Yokoyama M, Kono K, Shioda T, Sato H, et al. (2011) A single amino acid of human immunodeficiency virus type 2 capsid protein affects conformation of two external loops and viral sensitivity to TRIM5alpha. PLoS One 6: e22779.
32. Ode H, Yokoyama M, Kanda T, Sato H (2011) Identification of folding preferences of cleavage junctions of HIV-1 precursor proteins for regulation of cleavability. J Mol Model 17: 391–399.
33. Baker D, Sali A (2001) Protein structure prediction and structural genomics. Science 294: 93–96.
34. Case DA, Cheatham TE, 3rd, Darden T, Gohlke H, Luo R, et al. (2005) The Amber biomolecular simulation programs. J Comput Chem 26: 1668–1688.
35. Sato H, Kato K, Takebe Y (1999) Functional complementation of the envelope hypervariable V3 loop of human immunodeficiency virus type 1 subtype B by the subtype E V3 loop. Virology 257: 491–501.
36. Hachiya A, Aizawa-Matsuoka S, Tanaka M, Takahashi Y, Ida S, et al. (2001) Rapid and simple phenotypic assay for drug susceptibility of human immunodeficiency virus type 1 using CCR5-expressing HeLa/CD4(+) cell clone 1–10 (MAGIC-5). Antimicrob Agents Chemother 45: 495–501.
37. di Marzo Veronese F, Rahman R, Pal R, Boyer C, Romano J, et al. (1992) Delineation of immunoreactive, conserved regions in the external glycoprotein of the human immunodeficiency virus type 1. AIDS Res Hum Retroviruses 8: 1125–1132.
38. Simmonds P, Balfe P, Ludlam CA, Bishop JO, Brown AJ (1990) Analysis of sequence diversity in hypervariable regions of the external glycoprotein of human immunodeficiency virus type 1. J Virol 64: 5840–5850.
39. Burns DP, Desrosiers RC (1994) Envelope sequence variation, neutralizing antibodies, and primate lentivirus persistence. Curr Top Microbiol Immunol 188: 185–219.
40. Bonhoeffer S, Holmes SE, Nowak M (1995) Causes of HIV diversity. Nature 376: 125.
41. Lukashov VV, Kuiken CL, Goudsmit J (1995) Intrahost human immunodeficiency virus type 1 evolution is related to length of the immunocompetent period. J Virol 69: 6911–6916.
42. Buonaguro L, Tornesello ML, Buonaguro FM (2007) Human immunodeficiency virus type 1 subtype distribution in the worldwide epidemic: pathogenetic and therapeutic implications. J Virol 81: 10209–10219.
43. Brown LS, Kamikubo H, Zimanyi L, Kataoka M, Tokunaga F, et al. (1997) A local electrostatic change is the cause of the large-scale protein conformation shift in bacteriorhodopsin. Proc Natl Acad Sci U S A 94: 5040–5044.
44. Wu SR, Loving R, Lindqvist B, Hebert H, Koeck PJ, et al. (2010) Single-particle cryoelectron microscopy analysis reveals the HIV-1 spike as a tripod structure. Proc Natl Acad Sci U S A 107: 18844–18849.
45. White TA, Bartesaghi A, Borgnia MJ, Meyerson JR, de la Cruz MJ, et al. (2010) Molecular architectures of trimeric SIV and HIV-1 envelope glycoproteins on intact viruses: strain-dependent variation in quaternary structure. PLoS Pathog 6: e1001249.
46. Hu G, Liu J, Taylor KA, Roux KH (2011) Structural comparison of HIV-1 envelope spikes with and without the V1/V2 loop. J Virol 85: 2741–2750.
47. McLellan JS, Pancera M, Carrico C, Gorman J, Julien JP, et al. (2012) Structure of HIV-1 gp120 V1/V2 domain with broadly neutralizing antibody PG9. Nature 480: 336–343.
48. Shibata J, Yoshimura K, Honda A, Koito A, Murakami T, et al. (2007) Impact of V2 mutations on escape from a potent neutralizing anti-V3 monoclonal antibody during in vitro selection of a primary human immunodeficiency virus type 1 isolate. J Virol 81: 3757–3768.
49. Ogert RA, Lee MK, Ross W, Buckler-White A, Martin MA, et al. (2001) N-linked glycosylation sites adjacent to and within the V1/V2 and the V3 loops of dualtropic human immunodeficiency virus type 1 isolate DH12 gp120 affect coreceptor usage and cellular tropism. J Virol 75: 5998–6006.
50. Kwon YD, Finzi A, Wu X, Dogo-Isonagie C, Lee LK, et al. (2012) Unliganded HIV-1 gp120 core structures assume the CD4-bound conformation with regulation by quaternary interactions and variable loops. Proc Natl Acad Sci U S A 109: 5663–5668.
51. Sanchez R, Pieper U, Melo F, Eswar N, Marti-Renom MA, et al. (2000) Protein structure modeling for structural genomics. Nat Struct Biol 7 Suppl: 986–990.
52. Marti-Renom MA, Stuart AC, Fiser A, Sanchez R, Melo F, et al. (2000) Comparative protein structure modeling of genes and genomes. Annu Rev Biophys Biomol Struct 29: 291–325.
53. Ponder JW, Case DA (2003) Force fields for protein simulations. Adv Protein Chem 66: 27–85.
54. Case DA, Darden TA, Cheatham TE, Simmerling CL, Wang J, et al. (2006) AMBER 9. University of California: San Francisco.
55. Hornak V, Abel R, Okur A, Strockbine B, Roitberg A, et al. (2006) Comparison of multiple Amber force fields and development of improved protein backbone parameters. Proteins 65: 712–725.
56. Jorgensen WL, Chandrasekhar J, Madura JD, Impey RW, Klein ML (1983) Comparison of simple potential functions for simulating liquid water. J Chem Phys 79: 926–935.
57. Ryckaert JP, Ciccotti G, Berendsen HJC (1977) Numerical integration of the Cartesian equations of motion of a system with constraints: Molecular dynamics of n-alkanes. J Comput Phys 23: 327–341.
58. Matsushita S, Robert-Guroff M, Rusche J, Koito A, Hattori T, et al. (1988) Characterization of a human immunodeficiency virus neutralizing monoclonal antibody and mapping of the neutralizing epitope. J Virol 62: 2107–2114.
59. Yoshimura K, Harada S, Shibata J, Hatada M, Yamada Y, et al. (2010) Enhanced Exposure of Human Immunodeficiency Virus Type 1 Primary Isolate Neutralization Epitopes through Binding of CD4 Mimetic Compounds. J Virol.
60. Shiino T, Kato K, Kodaka N, Miyakuni T, Takebe Y, et al. (2000) A group of V3 sequences from human immunodeficiency virus type 1 subtype E non-syncytium-inducing, CCR5-using variants are resistant to positive selection pressure. J Virol 74: 1069–1078.
61. Motomura K, Oka T, Yokoyama M, Nakamura H, Mori H, et al. (2008) Identification of monomorphic and divergent haplotypes in the 2006 2007 norovirus GII/4 epidemic population by genomewide tracing of evolutionary history. J Virol 82: 11247–11262.
62. Oka T, Yokoyama M, Katayama K, Tsunemitsu H, Yamamoto M, et al. (2009) Structural and biological constraints on diversity of regions immediately upstream of cleavage sites in calicivirus precursor proteins. Virology 394: 119–129.
63. Shannon CE (1997) The mathematical theory of communication. 1963. MD Comput 14: 306–317.

Kono et al. Retrovirology 2010, 7:72
http://www.retrovirology.com/content/7/1/72

RETROVIROLOGY

RESEARCH Open Access

Multiple sites in the N-terminal half of simian immunodeficiency virus capsid protein contribute to evasion from rhesus monkey TRIM5α-mediated restriction

Ken Kono[1], Haihan Song[1], Masaru Yokoyama[2], Hironori Sato[2], Tatsuo Shioda[1], Emi E Nakayama[1*]

Abstract

Background: We previously reported that cynomolgus monkey (CM) TRIM5α could restrict human immunodeficiency virus type 2 (HIV-2) strains carrying a proline at the 120th position of the capsid protein (CA), but it failed to restrict those with a glutamine or an alanine. In contrast, rhesus monkey (Rh) TRIM5α could restrict all HIV-2 strains tested but not simian immunodeficiency virus isolated from macaque (SIVmac), despite its genetic similarity to HIV-2.

Results: We attempted to identify the viral determinant of SIVmac evasion from Rh TRIM5α-mediated restriction using chimeric viruses formed between SIVmac239 and HIV-2 GH123 strains. Consistent with a previous study, chimeric viruses carrying the loop between α-helices 4 and 5 (L4/5) (from the 82nd to 99th amino acid residues) of HIV-2 CA were efficiently restricted by Rh TRIM5α. However, the corresponding loop of SIVmac239 CA alone (from the 81st to 97th amino acid residues) was not sufficient to evade Rh TRIM5α restriction in the HIV-2 background. A single glutamine-to-proline substitution at the 118th amino acid of SIVmac239 CA, corresponding to the 120th amino acid of HIV-2 GH123, also increased susceptibility to Rh TRIM5α, indicating that glutamine at the 118th of SIVmac239 CA is necessary to evade Rh TRIM5α. In addition, the N-terminal portion (from the 5th to 12th amino acid residues) and the 107th and 109th amino acid residues in α-helix 6 of SIVmac CA are necessary for complete evasion from Rh TRIM5α-mediated restriction. A three-dimensional model of hexameric GH123 CA showed that these multiple regions are located on the CA surface, suggesting their direct interaction with TRIM5α.

Conclusion: We found that multiple regions of the SIVmac CA are necessary for complete evasion from Rh TRIM5α restriction.

Background

The host range of human immunodeficiency virus type 1 (HIV-1) is very narrow, being limited to humans and chimpanzees [1]. HIV-1 fails to replicate in activated CD4-positive T lymphocytes obtained from Old World monkeys (OWM) such as rhesus (Rh) [2,3] and cynomolgus (CM) monkeys [4,5]. Simian immunodeficiency virus (SIV) isolated from sooty mangabey (SIVsm) and SIV isolated from African green monkey (SIVagm) replicate in their natural hosts [6]. SIV isolated from a macaque monkey (SIVmac) evolved from SIVsm in captive macaques, and replicates efficiently in Rh [2,3] and CM [4,5] monkeys. Human immunodeficiency virus type 2 (HIV-2) is assumed to have originated from SIVsm as the result of zoonotic events involving monkeys and humans [7]. Previous studies have shown that HIV-2 strains vary widely in their ability to grow in cells of OWM such as baboon, and Rh and CM monkeys [8-12].

In 2004, the screening of a Rh cDNA library identified TRIM5α as a factor that confers resistance to HIV-1 infection [13]. Both Rh and CM TRIM5α proteins restrict HIV-1 infection but fail to restrict SIVmac [13,14]. In contrast, human TRIM5α is almost powerless

* Correspondence: emien@biken.osaka-u.ac.jp
[1]Department of Viral Infections, Research Institute for Microbial Diseases, Osaka University, 3-1 Yamada-oka, Suita, Osaka 565-0871, Japan
Full list of author information is available at the end of the article

to restrict the aforementioned viruses, but potently restricts N-tropic murine leukemia viruses (N-MLV) and equine infectious anemia virus [15-17].

TRIM5α is a member of the tripartite motif (TRIM) family of proteins, and consists of RING, B-box 2, coiled-coil, and SPRY (B30.2) domains [18]. Proteins with RING domains possess E3 ubiquitin ligase activity [19]; therefore, TRIM5α was thought to restrict HIV-1 by proteasome-dependent pathways. However, proteasome inhibitors do not affect TRIM5α-mediated HIV-1 restriction, even though HIV-1 late reverse transcribed products are generated normally [20-22]. TRIM5α is thus supposed to use both proteasome-dependent and -independent pathways to restrict HIV-1.

The intact B-box 2 domain is also required for TRIM5α-mediated antiviral activity, since TRIM5α restrictive activity is diminished by several amino acid substitutions in the B-box 2 domain [23,24]. TRIM5α has been shown to form a dimer [25,26], while the B-box 2 domain mediates higher-order self-association of Rh TRIM5α oligomers [27,28]. The coiled-coil domain of TRIM5α is important for the formation of homo-oligomers [29], and the homo-oligomerization of TRIM5α is essential for antiviral activity [30,31]. The SPRY domain is specific for an α-isoform among at least three splicing variants transcribed from the *TRIM5* gene. Soon after the identification of TRIM5α as a restriction factor of Rh, several studies found that differences in the amino acid sequences of the TRIM5α SPRY domain of different monkey species affect the species-specific restriction of retrovirus infection [14,32-39]. Studies on human and Rh recombinant TRIM5αs have shown that the determinant of species-specific restriction against HIV-1 infection resides in variable region 1 (V1) of the SPRY domain [32,33]. In the case of HIV-2 infection, we previously found that three amino acid residues of TFP at the 339th to 341st positions of Rh TRIM5α V1 are indispensable for restricting particular HIV-2 strains that are still resistant to CM TRIM5α [34].

The SPRY domain is thus thought to recognize viral cores. Biochemical studies have shown that TRIM5α associates with CA in detergent-stripped N-MLV virions [40] or with an artificially constituted HIV-1 core structure composed of the capsid-nucleocapsid (CA-NC) fusion protein in a SPRY domain-dependent manner [41]. Ylinen *et al.* mapped one of the determinants of Rh TRIM5α sensitivity to a loop between α-helices 4 and 5 (L4/5) of HIV-2 [42]. In the present study, we found that the 120th amino acid of HIV-2 CA, which is the determinant of CM TRIM5α sensitivity, also contributes to Rh TRIM5α susceptibility. Furthermore, studies on chimeric viruses between Rh TRIM5α-sensitive HIV-2 and -resistant SIVmac revealed that multiple regions in the N-terminal half of SIVmac CA including L4/5 contribute to the escape of SIVmac from Rh TRIM5α.

Methods

DNA constructs

The HIV-2 derivatives were constructed on a background of infectious molecular clone GH123 [43]. Construction of GH123/Q, the mutant GH123 possessing Q at the 120th position of CA protein, and SIVmac239/P, the mutant SIVmac239 possessing P at the 118th position of CA, were described previously [44]. The CA L4/5 of GH123 or GH123/Q was replaced with the corresponding segments of SIVmac239 CA using site-directed mutagenesis with the PCR-mediated overlap primer extension method [45], and the resultant constructs were designated GH123/CypS or GH123/CypS 120Q, respectively. The GH123 derivative with L4/5 of SIVmac239, Q at the 120th, and A at the 179th position of CA (GH123/CypS 120Q 179A) was generated by site-directed mutagenesis on a background of GH123/CypS 120Q.

Chimeric GH123 containing the whole region of SIVmac239 CA (GH/SCA) was generated by site-directed mutagenesis. Restriction enzyme sites *Ngo*M IV and *Xho* I, located in the LTR and p6 cording region, respectively, were used for DNA recombination. To obtain the *Ngo*M IV-*Xho* I fragment containing the CA region, we performed four successive PCR reactions using GH123 and SIVmac239 as templates. The primers used in these reactions were GH114F (5'-TTGGCCGGCACTGG-3'), SCA1For (5'-CCAGTACAACAAATAGG-3'), SCA1 Rev (5'-CCTATTTGTTGTACTGG-3'), SCA2 For (5'-GCTAGATTAATGGCCGAAGCCCTG-3'), SCA2 Rev (5'-CAGGGCTTCGGCCATTAATCTAGC-3'), and 2082R (5'-GACAGAGGACTTGCTGCAC-3').

The first PCR reaction used GH123 as a template and GH114F and GHSCA1 Rev as primers, the second used SIVmac239 as a template and GHSCA1 For and GHSCA2 Rev as primers, and the third used GH123 as a template and GHSCA2 For and 2082R as primers. The resultant 1st, 2nd, and 3rd fragments were used as templates in the fourth reaction with GH114F and 2082R as primers. The resultant *Ngo*M IV-*Xho* I fragment was transferred to GH123. GH/SCA derivatives GH/SCA N-G, GH/SCA VD, GH/SCA CypG, and GH/SCA TE were constructed by site-directed mutagenesis on a GH/SCA background.

To construct GH/NSCG, a GH123 derivative containing the N-terminal half (from 1st to 120th) of SIVmac239CA, we performed three successive PCR reactions. The first used GH/SCA as a template and GH114F and NSCA Rev (5'-GGGATTTTGTTGTCTGTACATCC-3') as primers, the second used GH123 as a

template and NSCA For (5'-GGATGTACAGACAA-CAAAATCCC-3') and 2082R as primers. The resultant 1st and 2nd fragments were used as templates in the third reaction with GH114F and 2082R as primers. The resultant *Ngo*M IV-*Xho* I fragment was transferred to GH123. The GH/NSCG derivative GH/GSG was constructed by site-directed mutagenesis on a GH/NSCG background.

Cells

The 293T (human kidney) and FRhK4 (Rh kidney; American Type Culture Collection, Manassas, VA) were cultured in Dulbecco's modified Eagle medium supplemented with 10% heat-inactivated fetal bovine serum (FBS). MT4, a human CD4 positive T cell line immortalized by human T cell leukemia virus type 1 [46], was maintained in RPMI 1640 medium containing 10% FBS.

Viral propagation

Virus stocks were prepared by transfection of 293T cells with HIV-2 GH123 derivatives using the calcium phosphate co-precipitation method. Viral titers were measured with the p27 RETROtek antigen ELISA kit (ZeptoMetrix, Buffalo, NY).

Recombinant Sendai virus (SeV) carrying Rh, CM, or CM SPRY(-) TRIM5α was described previously [14,34]. Green fluorescence protein (GFP) expressing HIV-1 carrying SIVmac239 L4/5 (HIV-1-L4/5-GFP) was prepared as described previously [47].

Viral infection

MT4 cells (2×10^5) were infected with SeV expressing each of the TRIM5αs, at a multiplicity of infection (MOI) of 10 plaque-forming units (pfu) per cell and incubated at 37°C for 9 h. Cells were then superinfected with 20 ng of p25 of HIV-2 GH123 or derivatives, or 20 ng of p27 of SIVmac239 or derivatives. Culture supernatants were collected periodically, and the levels of p25 or p27 were measured with the RETROtek antigen ELISA kit.

Particle purification and Western blot analysis

Culture supernatant of 293T cells transfected with plasmids encoding HIV-1 NL43 and HIV-2 GH123 derivatives was clarified using low-speed centrifugation. The resultant supernatants were layered onto a cushion of 20% sucrose (made in PBS) and centrifuged at 35,000 rpm for 2 h in a Beckman SW41 rotor. After centrifugation, the virion pellets were resuspended in PBS and applied to sodium dodecyl sulfate-polyacrylamide gel electrophoresis (SDS-PAGE). Virion-associated proteins were transferred to a PVDF membrane. CAs and cyclophilin A (CypA) were visualized with the serum from SIV-infected monkeys or the anti-CypA antibody (Affinity BioReagents, Golden, CO), respectively.

Saturation assay

HIV-2 or SIVmac derivative particles were prepared by co-transfection of the relevant plasmids with one encoding vesicular stomatitis virus glycoprotein (VSV-G) into 293T cells, and culture supernatants were collected two days after transfection. One day before infection, FRhK-4 cells were plated at a density of 2×10^4 cells per well in a 24-well plate. Prior to GFP virus infection, the cells were pretreated for 2 h with 800 ng of p25 of each of HIV-2 or SIVmac derivatives pseudotyped with VSV-G. Immediately after pretreatment, cells were washed and infected with 10 ng of p24 of the HIV-1-L4/5-GFP virus. Then, 2 h after infection, the inoculated GFP viruses were washed and the cells cultivated in fresh media. Two days after infection, GFP-positive cells were counted with a flow cytometer.

Molecular modeling of hexameric HIV-2 CA

The crystal structures of the HIV-2 CA N-terminal domain at a resolution of 1.25Å [PDB: 2WLV] [48], HIV-1 CA C-terminal domain at a resolution of 1.70Å (PDB code: 1A8O) [49], and hexameric HIV-1 CA at a resolution of 1.90Å [PDB:3H47] [50] were taken from the RCSB Protein Data Bank [51]. Three-dimensional (3-D) models of monomeric HIV-2 CA were constructed by the homology modeling technique using 'MOE-Align' and 'MOE-Homology' in the Molecular Operating Environment (MOE) version 2008.1002 (Chemical Computing Group Inc., Quebec, Canada) as described [44,52]. We obtained 25 intermediate models per one homology modeling in MOE, and selected those 3-D models which were intermediate with best scores according to the generalized Born/volume integral methodology [53]. The final 3-D models were thermodynamically optimized by energy minimization using an AMBER99 force field [54] combined with the generalized Born model of aqueous solvation implemented in MOE [55]. Physically unacceptable local structures of the optimized 3-D models were further refined on the basis of evaluation by the Ramachandran plot using MOE. The structures of hexameric HIV-2 CA were generated from the monomeric structures by MOE on the basis of the assembly information of hexameric HIV-1 CA crystal structures [50].

Results

The L4/5 loop of SIVmac239 CA and Q and A at the 120th and 179th positions of CA are not sufficient for HIV-2 to evade Rh TRIM5α-mediated restriction

Previously, we evaluated the antiviral effect of CM and Rh TRIM5α and found that CM TRIM5α could restrict

HIV-2 GH123 carrying P at the 120th position of CA, but failed to restrict the HIV-2 GH123 mutant in which P was replaced with Q (GH123/Q) [44] (Figure 1A). In contrast, Rh TRIM5α could restrict both viruses [34] (Figure 2A and 2B). Although CA of HIV-2 GH123 and SIVmac239 share more than 87% amino acid identity (Figure 1B), CM and Rh TRIM5αs failed to restrict SIVmac239 (Figure 2C).

Since wild type SIVmac239 possesses Q at the 118th position of CA (analogous to the 120th position of GH123 CA), we constructed mutant SIVmac239 carrying P at the 118th position (SIVmac239/P), and found

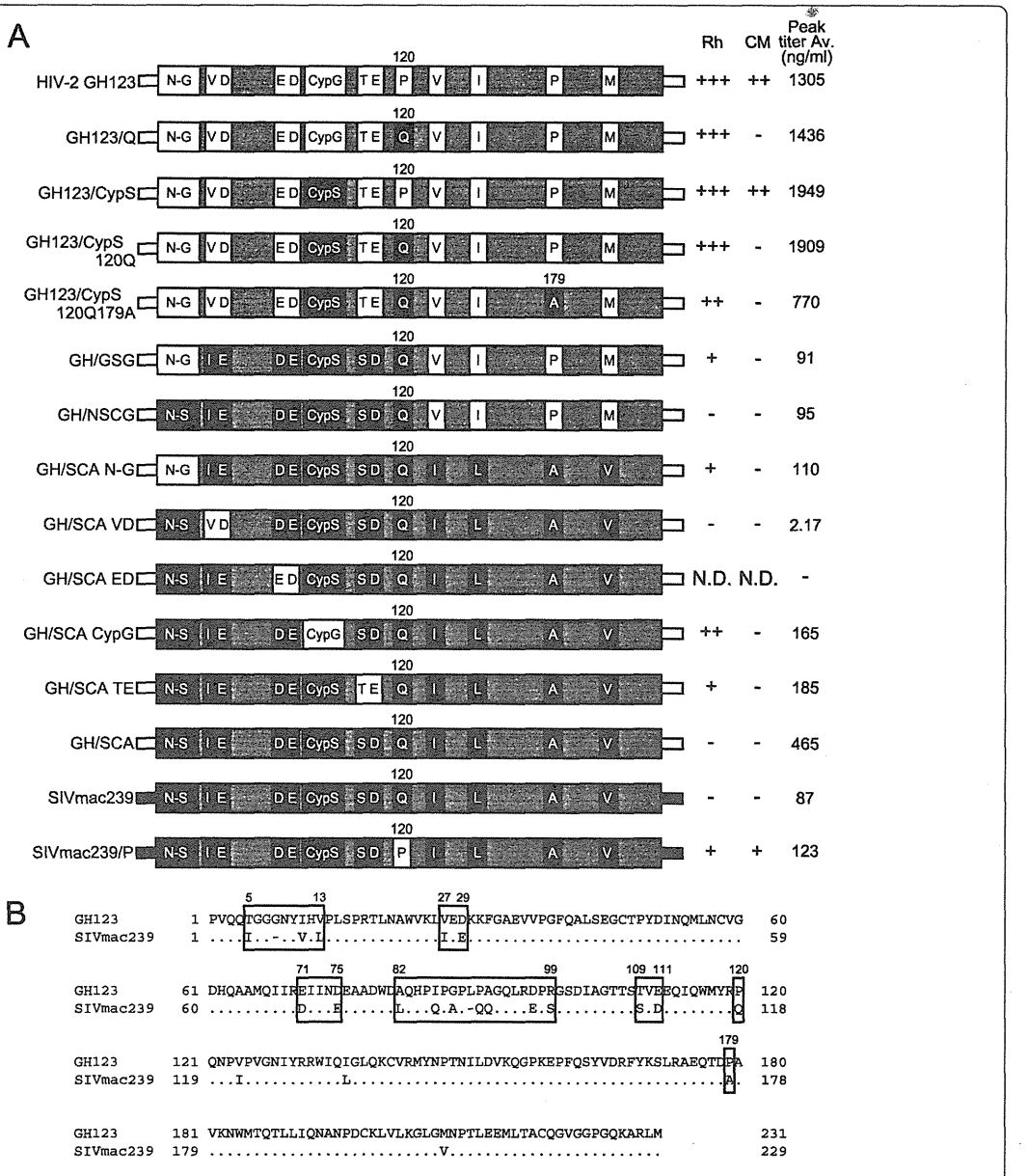

Figure 1 Schematic representation of chimeric viral CAs. (A) White and black bars denote HIV-2 GH123 and SIVmac239 sequences, respectively. +++, ++, +, and - denote more than 1000-fold, 100- to 1000-fold, 5- to 100-fold, and less than 5-fold suppression of viral growth, respectively, compared with viral growth in the presence of negative control CM SPRY(-) TRIM5α on day 6. Peak titer Av. denotes average titers in the presence of CM SPRY(-) TRIM5α on day 6 of two independent experiments. (B) Alignments of amino acid sequences of GH123 and SIVmac239 CAs. Dots denote amino acid residues identical to one of the GH123 CA and dashes denote lack of an amino acid residue present in GH123 CA. Boxes show the regions replaced between GH123 and SIVmac239.

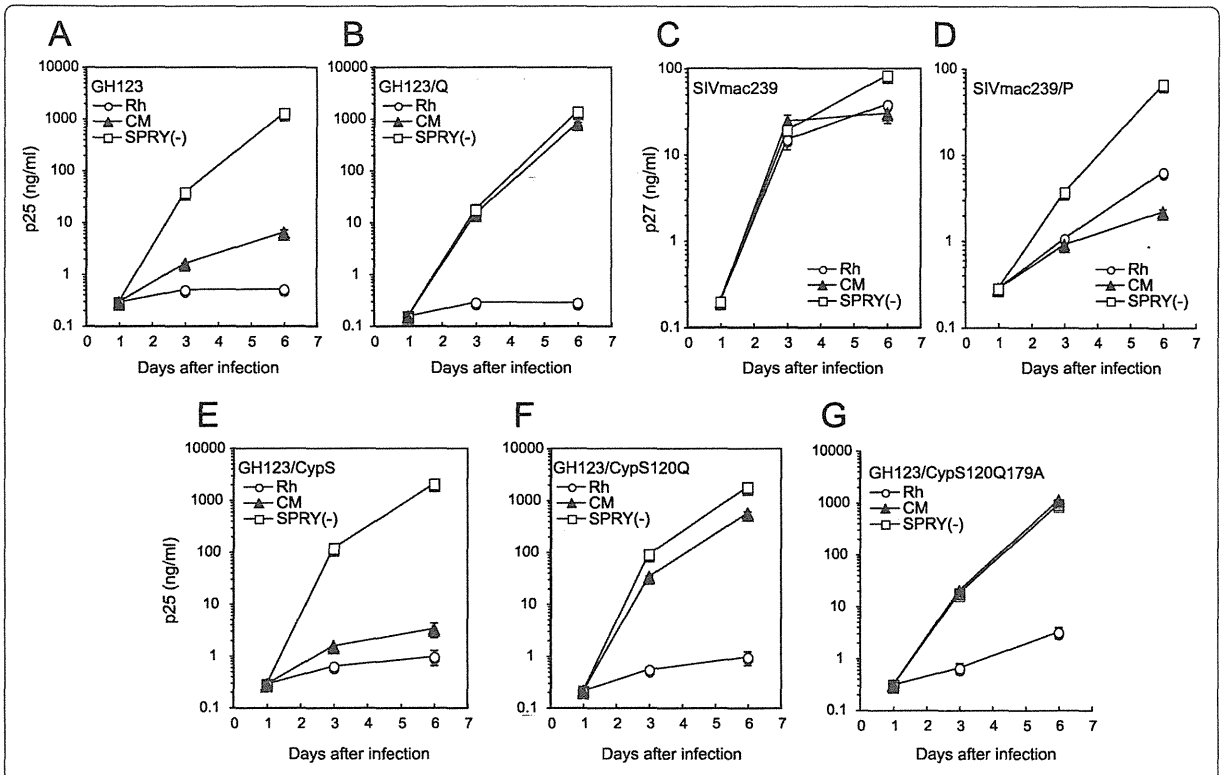

Figure 2 MT4 cells were infected with recombinant SeV expressing Rh (white circles), CM (black triangles), or CM SPRY(-) (white squares) TRIM5α. Nine hours after infection, cells were superinfected with GH123, SIVmac239 or their derivative viruses. Culture supernatants were separately assayed for levels of p25 from GH123 or p27 from SIVmac239. Error bars show actual fluctuations between levels of p25 or p27 in duplicate samples. A representative of two independent experiments is shown.

that CM and Rh TRIM5αs could restrict the mutant virus [44] (Figure 2D). These results indicate that Q at the 118th position of CA is required to evade restriction by CM and Rh TRIM5αs, although Rh TRIM5α could restrict GH123/Q. In the case of Rh TRIM5α, it has been reported that Rh TRIM5α sensitivity determinants lie in the loop between α-helices 4 and 5 of CA protein, equivalent to the cyclophilin A (CypA) binding loop of HIV-1 [42]. This conclusion was made after Rh TRIM5α restricted SIVmac-based SIV H2L in which the L4/5 was replaced with that of HIV-2. However, when we constructed a GH123 derivative in which L4/5 was replaced with that of SIVmac239 (GH123/CypS), the reciprocal virus of SIV H2L, we found that Rh TRIM5α still restricted this virus very well (Figure 2E), indicating that SIVmac239 L4/5 alone is not sufficient for HIV-2 to evade Rh TRIM5α restriction.

We then constructed a GH123 derivative with L4/5 of SIVmac239 (CypS) and Q at the 120th position of CA (GH123/CypS 120Q). Contrary to our expectations, Rh TRIM5α still fully restricted this virus (Figure 2F). Since we previously found that the amino acid change at the 179th position of HIV-2 CA correlated with plasma viral load in infected individuals [56], we next replaced P at the 179th position of GH123/CypS 120Q CA with alanine (A) of SIVmac239 CA analogous to the 179th position of GH123 CA to generate GH123/CypS 120Q179A. However, Rh TRIM5α also completely restricted this virus (Figure 2G). The peak titers of GH123/CypS 120Q and GH123/CypS 120Q179A in cells expressing Rh TRIM5α were approximately 1000 times (+++ in Figure 1) and 300 times (++ in Figure 1), respectively, lower than those in cells expressing CM TRIM5α lacking the SPRY domain, CM SPRY (-) TRIM5α, a negative control for functional TRIM5α (Figure 2F and 2G). Although this result suggests that the 179th amino acid slightly contributes to evade Rh TRIM5α, it is clear that L4/5 of SIVmac239 CA and Q at the 120th and A at the 179th positions of CA were insufficient to evade Rh TRIM5α-mediated restriction.

In the case of CM TRIM5α, viruses carrying P at the 120th position (GH123, GH123/CypS, and SIVmac239/P) were restricted by CM TRIM5α, whereas all other viruses bearing Q (GH123/Q, GH123/CypS 120Q, GH123/CypS 120Q179A, and SIVmac239) were not (Figures 1 and 2). These results are in good agreement

with our previous conclusion that glutamine at the 120th position of HIV-2 CA alone is sufficient to evade CM TRIM5α restriction [34,44].

The N-terminal half of SIVmac239 CA is sufficient to evade Rh TRIM5α

To confirm that CA contains all determinants for restriction by Rh TRIM5α, we constructed a chimeric GH123 containing the whole region of SIVmac239 CA (GH/SCA). This virus could grow in the presence and absence of Rh TRIM5α (Figures 1 and 3A), clearly excluding the possibility that some of the determinants lie outside the CA. We then generated a chimeric GH123 containing the N-terminal half (from the 1st to 120th) of SIVmac239 CA (GH/NSCG) to further narrow down the determinant for restriction by Rh TRIM5α. Although GH/NSCG grew to lower titers than GH/SCA, even in the absence of Rh TRIM5α, this virus could also grow in the presence of Rh TRIM5α (Figures 1 and 3B). These results suggest that the N-terminal half of SIVmac239 CA is almost sufficient to evade Rh TRIM5α, even though the 179th amino acid of the C-terminal half possessed a slight effect of restriction.

Multiple sites in the N-terminal half of SIVmac239 CA contribute to evasion from restriction by Rh TRIM5α

In the N-terminal half of GH123 CA, 19 amino acid residues differ from those of SIVmac239. We grouped these differences into six regions as shown by boxes in Figure 1B, and evaluated their contribution to evasion from Rh TRIM5α by replacing each region of GH/SCA with the corresponding region of GH123. Rh TRIM5α completely restricted the GH/SCA derivative with the GH123 L4/5 (CypG) (GH/SCA CypG) (Figures 1 and 3C), consistent with a previous study [42]. Rh TRIM5α moderately restricted the GH/SCA derivative with threonine (T) and glutamic acid (E) of GH123 at the 109th and 111th positions, respectively (GH/SCA TE) (Figures 1 and 3D). These results suggest that not only L4/5 but also the 107th and 109th of amino acid residues of SIVmac239 CA (analogous to the 109th and 111th of GH123 CA) contribute to evasion from restriction by Rh TRIM5α.

Moreover, Rh TRIM5α slightly but significantly restricted the GH/SCA derivative with the GH123 N-terminal portion from the 5th to 13th amino acid residues (N-G) (GH/SCA N-G) (Figures 1 and 3E) ($p < 0.05$, t-test, n = 4), indicating that the SIVmac239 N-terminal portion from 5th to 12th (N-S) (analogous to N-G) is also important in evasion from Rh TRIM5α. Consistent with this result, Rh TRIM5α which failed to restrict GH/NSCG, could restrict the GH/NSCG

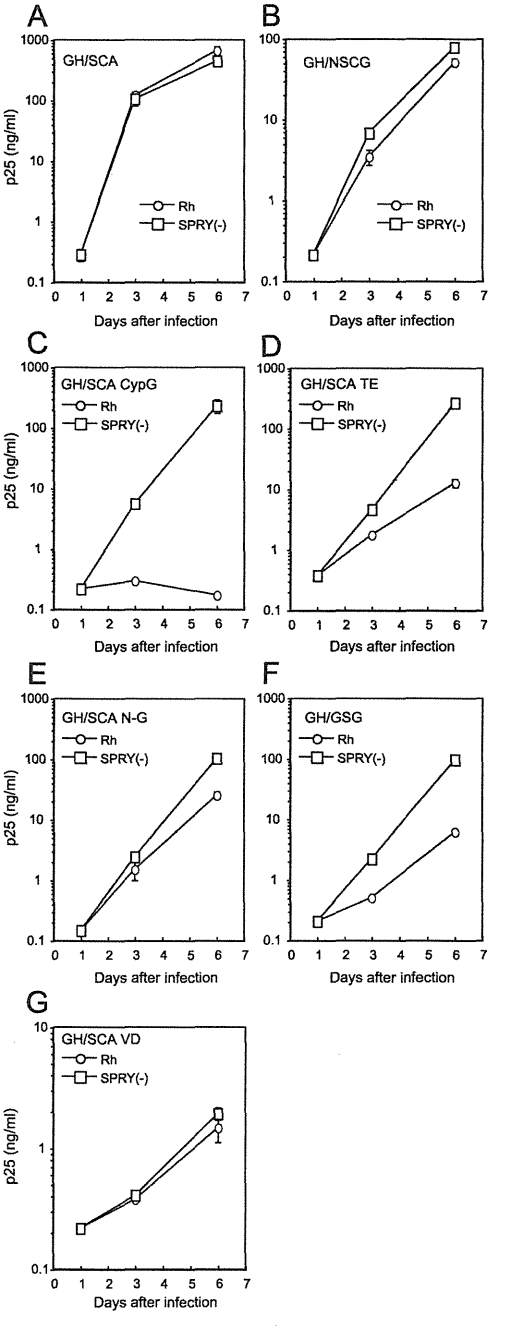

Figure 3 MT4 cells were infected with recombinant SeV expressing Rh (white circles) or CM SPRY(-) (white squares) TRIM5α. Nine hours after infection, cells were superinfected with GH/SCA (A), GH/NSCG (B) or GH/SCA derivatives (C-G). Culture supernatants were separately assayed for levels of p25. Error bars show actual fluctuations between levels of p25 in duplicate samples. A representative of two independent experiments is shown.

derivative with N-G (GH/GSG) (Figures 1 and 3F). On the other hand, Rh TRIM5α failed to restrict the GH/SCA derivative with the valine (V) and aspartic acid (D) of GH123 at the 27th and 29th positions, respectively (GH/SCA VD) (Figures 1 and 3G). It should be noted, however, that the growth capability of GH/SCA VD in MT4 cells was extremely low even in the absence of TRIM5α (Figure 3G), and further studies are necessary to address the contribution of this region to viral sensitivity to Rh TRIM5α. Similarly, the GH/SCA derivative with glutamic acid (E) and D of GH123 at the 71st and 75th positions (GH/SCA ED) (Figure 1) did not grow in MT4 cells expressing CM SPRY (-) TRIM5α, thus, we were unable to evaluate the effect of these sites. Taken together, we conclude that multiple sites in the N-terminal half of SIVmac239 CA (N-S, CypS (L4/5), and the 107th, 109th, and 118th amino acid residues) contribute to evasion from restriction by Rh TRIM5α.

We previously reported that a mutant CM TRIM5α possessing TFP instead of Q at the 339th position (CM Q-TFP TRIM5α) potently restricted GH123/Q [34]. In the present study, CM Q-TFP TRIM5α showed nearly the same spectrum of virus restriction as Rh TRIM5α as it completely restricted GH/SCA CypG, moderately restricted GH/SCA TE and SIVmac239/P, and only slightly restricted GH/SCA N-G (data not shown). These results indicate that the virus restriction specificity of Rh TRIM5α is highly dependent on the three amino acid residues 339th-TFP-341st.

CypA was not incorporated into GH123, SIVmac239 or their derivative virus particles

It has been reported that CypA was incorporated into group M HIV-1, but not HIV-2 or SIVmac particles [57]. To confirm that the replacement of CA between GH123 and SIVmac239 did not augment CypA incorporation, we performed Western blot analysis of viral particles from GH123, SIVmac239, and their derivatives. As shown in Figure 4 (upper panel), CypA proteins were clearly detected in the particles of HIV-1 NL43 but not in those of GH123, GH/SCA, GH/SCA CypG or SIVmac239, although the amount of their CA proteins was almost comparable (Figure 4, lower panel). This result indicates that the replacement between GH123 and SIVmac239 did not augment their CypA incorporation ability.

Rh TRIM5α-resistant HIV-2 derivative virions showed impaired saturation activity to TRIM5α in Rh cells

It is known that TRIM5α-mediated restriction of retroviral infection is saturated when cells are exposed to high doses of restriction-sensitive viral particles [58-61]. To determine whether the amino acid substitutions we generated would affect the viral ability to saturate

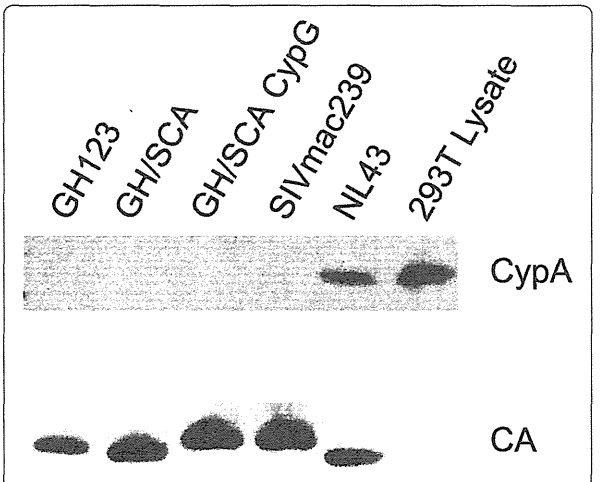

Figure 4 Western blot analysis of CA and CypA in particles of GH123, SIVmac239 and their derivatives. Viral particles from HIV-1 NL43, HIV-2 GH123, SIVmac239, and their derivatives were purified by ultracentrifugation through a 20% sucrose cushion. A total of 120 ng of p24 of HIV-1, p25 of HIV-2 GH123 derivatives or p27 of SIVmac239 derivatives was applied for gel electropholesis. Cyp A (upper panel) and CA (lower panel) were visualized by Western blotting (WB) using an anti-CypA antibody and serum from a SIV-infected monkey, respectively.

TRIM5α restriction, Rh FRhK4 cells were pre-treated with equal amounts of VSV-G pseudotyped HIV-2 GH123, SIVmac239, and their derivative viruses. The pretreated cells were then infected with VSV-G pseudotyped GFP expressing HIV-1 carrying SIVmac239 L4/5 (HIV-1-L4/5S-GFP) [47], since we wanted to exclude the effects of endogenous CypA on GFP-expressing virus in FRhK4 cells. The susceptibility of particle-treated cells to virus infection was determined by the percentage of GFP-positive cells.

Cells treated with HIV-2 GH123 particles showed enhanced susceptibility to HIV-1 infection compared with non-treated cells (Figure 5), demonstrating that TRIM5α in FRhK4 cells was saturated by the high dose of the particles. In contrast, cells treated with SIVmac239 particles showed very low levels of enhancement. Cells treated with particles carrying GH123/Q showed similar levels of enhanced susceptibility to HIV-1 infection to those of HIV-2 GH123, while cells treated with particles of GH123/CypS, GH123/CypS 120Q, GH/SCA CypG or SIVmac239/P showed intermediate levels of enhancement (Figure 5).

On the other hand, cells treated with particles carrying GH/NSCG, GH/SCA, and GH/SCA N-G showed similar levels of enhancement of HIV-1 susceptibility to those of SIVmac239 (Figure 5). These results are roughly consistent with our data shown in Figures 2 and 3, but there are two differences. First, Rh TRIM5α could

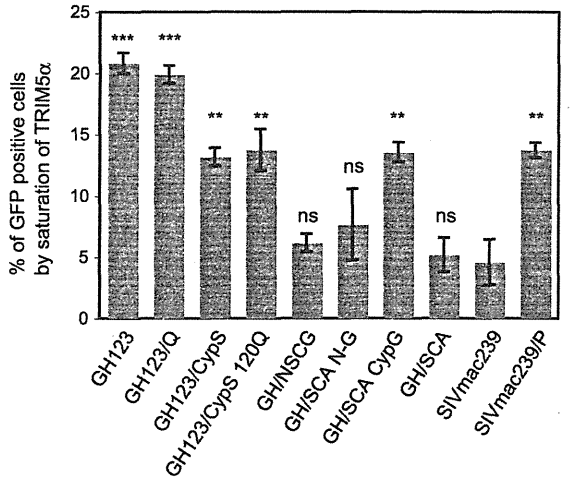

Figure 5 Activity of GH123, SIVmac239, and their derivatives to saturate TRIM5α in Rh cells. (A) Rh FRhK-4 cells were pretreated with equal amounts of VSV-G pseudotyped particles (800 ng of p25 or p27) of GH123, GH123/Q, GH123/CypS, GH123/CypS 120Q, GH/NSCG, GH/SCA N-G, GH/SCA CypG, GH/SCA, SIVmac239 or SIVmac239/P for 2 h. Cells were then infected with the VSV-G pseudotyped GFP-expressing HIV-1 vector carrying SIVmac L4/5. Data from triplicate samples (means ± SD) expressed as % GFP positive cells subtracted with the value of mock-treated cells (24.88%) are shown. Statistical significance of differences was calculated using the *t*-test. Asterisks above bars show differences between indicated viruses and SIVmac239. ***, $P < 0.001$; **, $P < 0.01$; ns, not significant. The statistical significance of differences between GH123 and GH123/CypS and that between GH123 and GH/SCA CypG were both < 0.001.

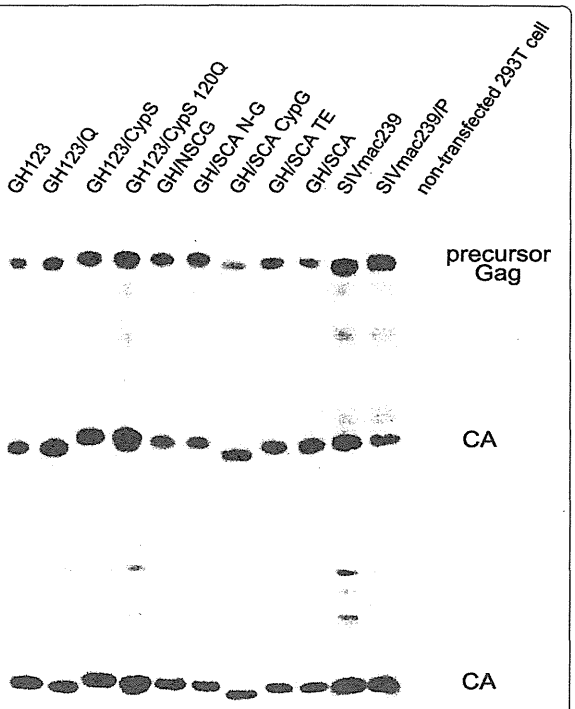

Figure 6 Western blot analysis of lysates of viral producer cells and viral particles. Viral proteins in the lysate of equal number of viral producer cells (upper panel) and particle fraction of equal volume of culture supernatant of viral producer cells (lower panel) were visualized by WB using serum from an SIV-infected monkey.

completely restrict GH123/CypS and GH123/CypS 120Q (Figure 2), while particles of these viruses showed decreased levels of enhancement compared with those of GH123 or GH123/Q (Figure 5). Second, Rh TRIM5α could slightly restrict GH/SCA N-G (Figure 3E), while particles of this virus failed to saturate Rh TRIM5α (Figure 5). Although the precise reasons for these differences are unclear at present, similar differences were previously reported in HIV-1 CA mutant constructs, and might be due to differences in core stability among mutant viral particles [62]. Nevertheless, our data in Figure 5 clearly indicate the importance of L4/5 (compare GH123 with GH123/CypS, GH/SCA with GH/SCA CypG) and other CA regions (compare GH123 with GH/SCA CypG, SIVmac239 with SIVmac239/P) in the viral ability to saturate TRIM5α in Rh FRhK4 cells, and suggest that the multiple sites in the N-terminal half of GH123 CA affect its binding to Rh TRIM5α.

Finally, we checked viral release and maturation/processing of GH123, SIVmac239, and their derivative viruses by a western blot for the lysate of viral producer cells (Figure 6, upper panel) and viral particles (Figure 6, lower panel), since viral maturation is essential for TRIM5α recognition. CA proteins in the cells and released viral particles were clearly detected. CAs with SIVmac239 L4/5 showed slightly reduced mobility compared with those with GH123 L4/5. Although there were small differences in the amounts of CA among viruses tested, there was no difference in the ratio of intracellular CA to those in the released viral particles. It should be also mentioned that there was no difference in the ratio of Gag precursors to processed CA in the viral producer cells. These results indicated that viral release and maturation/processing of the derivative viruses occurred normally.

Structural model of HIV-2 GH123 CA

To gain a structural insight into the mechanisms by which Rh TRIM5α recognizes HIV-2 CA, three-dimensional (3-D) models of monomeric and hexameric HIV-2 GH123 CA were constructed using homology-modeling based on the crystal structures of the HIV-2 CA N-terminal domain [48], HIV-1 CA C-terminal domain [49], and the hexameric HIV-1 CA [50]. All amino acid residues conferring sensitivity to Rh TRIM5α restriction (N-G, CypG (L4/5), the 109th T, 111th E, and 120th P) are located on the surface of CA

(Figure 7A, C and 7D), suggesting that these positions are involved in interaction with Rh TRIM5α. On the other hand, amino acid residues that impaired viral growth in the absence of TRIM5α (27th V, 29th D, 71st E, and 75th D) are located on the side of CA (Figure 7A and 7D). Although we were unable to determine the effect of these amino acid residues on viral sensitivity to Rh TRIM5α restriction, the structural models suggest that these sites are buried inside multimerized CA. It is therefore unlikely that they are involved in the direct interaction of CA with Rh TRIM5α.

Discussion

A previous study on the recombination between HIV-2 ROD and SIVmac showed that the CA region corresponding to the CypA binding loop of HIV-1 (L4/5) is

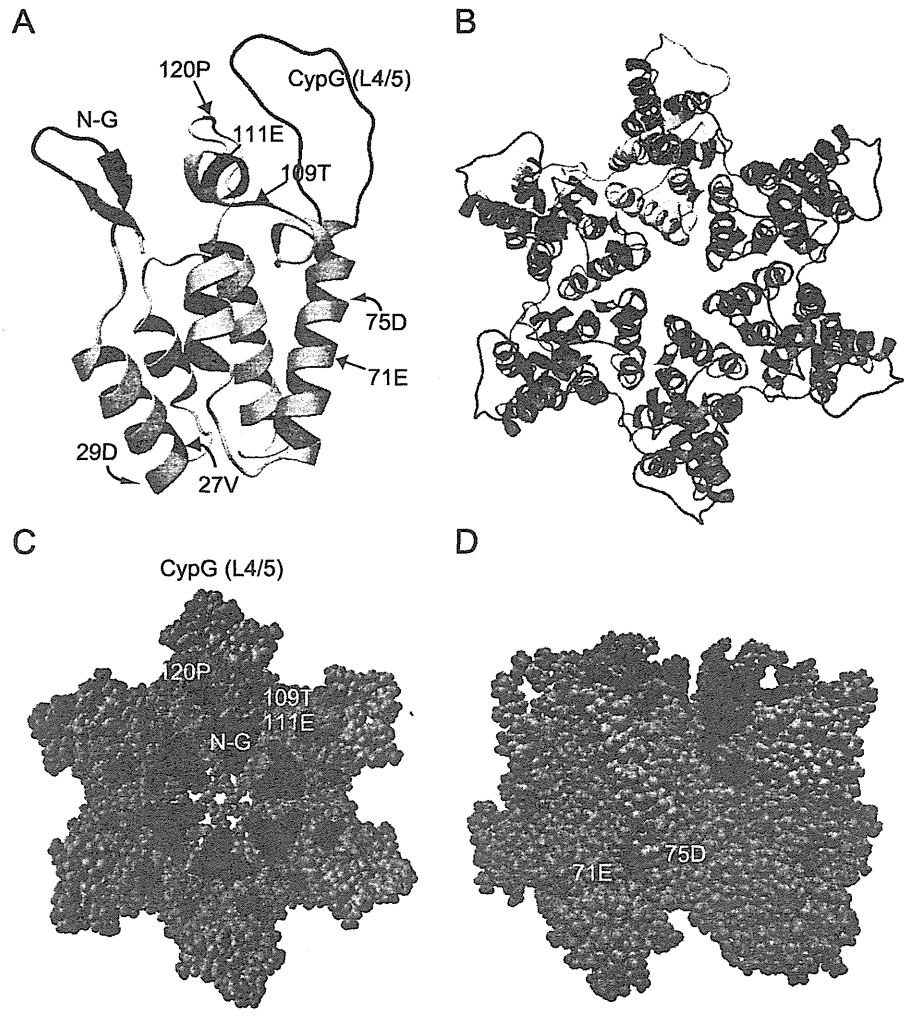

Figure 7 Three-dimensional structural models of GH123 CA. (A) Structure of the N-terminal half of CA monomer. The model was constructed by homology-modeling using "MOE-Align" and "MOE-Homology" in the Molecular Operating Environment (MOE) as described previously [73,74]. N-G, dark purple; the 27thV and the 29thD, pink; Cyp G (L4/5), orange; the 71stE, green; the 75thD, light purple; the 109th T, dark blue; the 111th E, light blue; and the 120th P, red. The structure of CA hexamer from the top (B and C) and side (D) is shown.

the determinant for susceptibility to Rh TRIM5α [42]. A subsequent study on HIV-1 and SIVagmTAN showed that the loop between helices 6 and 7 (L6/7) also contributes to Rh TRIM5α susceptibility [63]. In the present study, we showed that the L4/5 and the 120th amino acids located in L6/7 were required but not sufficient for HIV-2 to evade Rh TRIM5α-mediated restriction.

In addition to L4/5 and L6/7, we found that the N-terminal portion (from the 5th to 12th amino acid residues), and 107th and 109th amino acid residues in α-helix 6 of SIVmac239 CA are required for Rh TRIM5α evasion. The 3-D models of CA showed that the analogous regions of GH123 CA are located on the surface of the CA core structure, suggesting that these sites are involved in the direct interaction of CA with Rh TRIM5α. Our results are in good agreement with a previous report in which the HIV-1 derivative with an entire CA and Vif of SIVmac239 could replicate in Rh cells [64]. In addition, we observed that the HIV-1 derivative with L4/5 and L6/7 of CA and Vif of SIVmac239 (NLScaVR6/7S) that replicates in CM cells [47] failed to replicate in Rh cells (Kuroishi et al., unpublished data).

The growth ability of GH123 was higher than that of SIVmac239 in SeV-infected MT4 cells, but that of many GH123 derivatives with SIVmac239 CA sequences was lower than that of the parental GH123 and comparable with that of SIVmac239 (Figures 1, 2, and 3). However, GH/SCA VD replicated very poorly and GH/SCA ED did not replicate at all. These results were reproducible using the viruses produced with independent plasmid clones, after which Gag processing of these viruses occurred normally (data not shown). As shown in Figure 7, the 27th V and 29th D are in α-helix 1, and the 71st E and 75th D are in α-helix 4. It is possible that the amino acid changes at these sites are harmful for the formation of a multimerized viral core. Supporting this notion, the 27th V and 71st E are highly conserved among different HIV-2 strains in the Los Alamos sequence database. Furthermore, the 71st E and 75th D are located on the lateral side of the CA hexametric structure (Figure 7D), and thus it is possible that these amino acid residues associate with the neighboring CA hexamer. It is thus interesting to know the impact of such amino acid changes on viral core formation.

It has been reported that the CypA-CA interaction renders HIV-1 more susceptible to Rh TRIM5α restriction [65-68]. We found that HIV-2 CA L4/5 corresponding to the CypA binding loop of HIV-1 had the biggest impact on Rh TRIM5α susceptibility, although we could not detect CA-CypA binding (Figure 4). Braaten *et al.* also reported that neither HIV-2 nor SIV recruits CypA into their cores, and that drugs that block CA-CypA interaction have no effect on the titers of these viruses [57]. CA crystal structures of human T-cell lymphotropic virus type 1 [PDB: 1QRJ] [69] and equine infectious anemia virus [PDB: 1EIA] [70] possess an exposed loop directed to the surface of the CA core structure, similar to the HIV-1 CypA binding loop, while retroviruses such as B-tropic murine leukemia virus [PDB: 3BP9] [71] and Jaagsiekte sheep retrovirus [PDB: 2V4X] [72] do not. It is reasonable to assume that this HIV-2 loop would interact with certain host factors other than CypA, and consequently is an attractive target for TRIM5α.

The differences in the L4/5 amino acid sequence among different strains of HIV-2, SIVmac, and SIVsmm are shown in Figure 8. Of these, SIVmac-specific amino acid residues are the 88th A, 90th-QQΔ-92nd, and 99th S (Figure 8 boxes). Ylinen *et al.* reported that SIVmac QQ LPA, the mutant SIVmac containing HIV-2-specific LPA instead of QQ at the 90th to 92nd positions, was still not restricted by Rh TRIM5α [42], suggesting that the 88th and 99th amino acids or all amino acid substitutions in L4/5 between SIVmac and HIV-2 are involved in resistance to Rh TRIM5α restriction.

We previously reported that the TFP motif in the SPRY domain of Rh TRIM5α is important in restriction

```
                    82                                  99
H2A GH123           AQHPIPGPLPAGQLRDPR
H2A ROD             V.....|.|...|...E.|.
H2A UC2             .....|.|...|.....|.
H2A ALI             VA....|.|...|...E.|.
H2A D194            .....|.|...|.....|.
H2A BEN             S.....|.|...|.....|.
H2B KR020           V.....|.|...|.....|.
H2B UC1             Q.....|.|...|.....|.
H2U 12034           T...NQ|.|P..|...E.|.

MAC 239             L...Q.A.QQ-...E.S
MAC 95058           L...Q.A.QQ-.....S
MAC NN142           L...QQA.QQ-.....S
MAC MNE8            L...QQA.QQ-.....S

SMM PGM53           L...Q.|.|I..|.....|.
SMM SME543          L...Q.|.|...|...E.|.
SMM PBJ14           L...Q.|.|I.P|...E.|.
```

Figure 8 Alignments of amino acid sequences of the CA L4/5 region of HIV-2, SIVmac, and SIVsmm selected from the Los Alamos databases. Dots denote the amino acid identical to one of the GH123 CA and dashes denote lack of an amino acid residue that is present in GH123 and other viruses. Boxes show the site of SIVmac-specific amino acid residues. H2A, B, and U represent HIV-2 group A, B, and U, respectively. MAC represents SIVmac, and SMM denotes SIVsmm.

of HIV-2 strains that are not restricted by CM TRIM5α [34]. In the present study, we confirmed that this motif is both necessary and sufficient to restrict various HIV-2-SIVmac chimeras that are restricted by Rh TRIM5α. If the TFP motif in the SPRY domain of Rh TRIM5α is directly involved in interaction with viral CA, it is not clear why multiple regions of SIVmac239 are necessary for evasion from TRIM5α with a TFP motif. We previously constructed the 3-D structural model of the SPRY domain [36] using homology modeling. It would therefore be of interest to construct a 3-D binding model of CA and TRIM5α, and to understand how the 339th-TFP-341st motif of Rh TRIM5α affects recognition of the CAs that differ at multiple positions.

Conclusion

We found that multiple regions of the SIVmac CA, not only L4/5 and the 118th amino acid but also the N-terminal portion (from the 5th to 12th amino acid residues), and the 107th and 109th amino acid residues, are necessary for complete evasion from Rh TRIM5α restriction.

Acknowledgements

We thank Ayumu Kuroishi for providing a saturation assay protocol, Tadashi Miyamoto for helping with experiments, and Setsuko Bandou and Noriko Teramoto for their assistance. This work was supported by grants from the Health Science Foundation, the Ministry of Education, Culture, Sports, Science, and Technology, the Ministry of Health, Labour and Welfare, Japan, and the Japan Society for the Promotion of Science.

Author details

[1]Department of Viral Infections, Research Institute for Microbial Diseases, Osaka University, 3-1 Yamada-oka, Suita, Osaka 565-0871, Japan. [2]Laboratory of Viral Genomics, Pathogen Genomics Center, National Institute of Infectious Diseases, Gakuen 4-7-1, MusashiMurayama-shi, Tokyo, 208-0011, Japan.

Authors' contributions

KK and HS performed experiments. EEN and TS participated in its design. MY and HS carried out computational analysis. KK, EEN, HS and TS drafted the manuscript. All authors read and approved the final manuscript.

Authors' information

KK is a research fellow of the Japan Society for the Promotion of Science. HS was a PhD student of Osaka University. HS is a chief of Laboratory of Viral Genomics, Pathogen Genomics Center, National Institute of Infectious Diseases, Japan; and MY is a staff of this laboratory. TS is a professor, and EEN is an assistant professor of Research Institute for Microbial Diseases, Osaka University.

Competing interests

The authors declare that they have no competing interests.

Received: 9 June 2010 Accepted: 8 September 2010
Published: 8 September 2010

References

1. Gao F, Bailes E, Robertson DL, Chen Y, Rodenburg CM, Michael SF, Cummins LB, Arthur LO, Peeters M, Shaw GM, Sharp PM, Hahn BH: **Origin of HIV-1 in the chimpanzee Pan troglodytes troglodytes.** *Nature* 1999, **397**:436-441.
2. Shibata R, Sakai H, Kawamura M, Tokunaga K, Adachi A: **Early replication block of human immunodeficiency virus type 1 in monkey cells.** *J Gen Virol* 1995, **76(Pt 11)**:2723-2730.
3. Himathongkham S, Luciw PA: **Restriction of HIV-1 (subtype B) replication at the entry step in rhesus macaque cells.** *Virology* 1996, **219**:485-488.
4. Akari H, Mori K, Terao K, Otani I, Fukasawa M, Mukai R, Yoshikawa Y: **In vitro immortalization of Old World monkey T lymphocytes with Herpesvirus saimiri: its susceptibility to infection with simian immunodeficiency viruses.** *Virology* 1996, **218**:382-388.
5. Akari H, Nam KH, Mori K, Otani I, Shibata H, Adachi A, Terao K, Yoshikawa Y: **Effects of SIVmac infection on peripheral blood CD4+CD8+ T lymphocytes in cynomolgus macaques.** *Clin Immunol* 1999, **91**:321-329.
6. VandeWoude S, Apetrei C: **Going wild: lessons from naturally occurring T-lymphotropic lentiviruses.** *Clin Microbiol Rev* 2006, **19**:728-762.
7. Hahn BH, Shaw GM, De Cock KM, Sharp PM: **AIDS as a zoonosis: scientific and public health implications.** *Science* 2000, **287**:607-614.
8. Castro BA, Nepomuceno M, Lerche NW, Eichberg JW, Levy JA: **Persistent infection of baboons and rhesus monkeys with different strains of HIV-2.** *Virology* 1991, **184**:219-226.
9. Fujita M, Yoshida A, Sakurai A, Tatsuki J, Ueno F, Akari H, Adachi A: **Susceptibility of HVS-immortalized lymphocytic HSC-F cells to various strains and mutants of HIV/SIV.** *Int J Mol Med* 2003, **11**:641-644.
10. Castro BA, Barnett SW, Evans LA, Moreau J, Odehouri K, Levy JA: **Biologic heterogeneity of human immunodeficiency virus type 2 (HIV-2) strains.** *Virology* 1990, **178**:527-534.
11. Locher CP, Witt SA, Herndier BG, Abbey NW, Tenner-Racz K, Racz P, Kiviat NB, Murthy KK, Brasky K, Leland M, Levy JA: **Increased virus replication and virulence after serial passage of human immunodeficiency virus type 2 in baboons.** *J Virol* 2003, **77**:77-83.
12. Locher CP, Blackbourn DJ, Herndier BG, Reyes-Teran G, Barnett SW, Murthy KK, Levy JA: **Transient virus infection and pathogenesis of a new HIV type 2 isolate, UC12, in baboons.** *AIDS Res Hum Retroviruses* 1998, **14**:79-82.
13. Stremlau M, Owens CM, Perron MJ, Kiessling M, Autissier P, Sodroski J: **The cytoplasmic body component TRIM5alpha restricts HIV-1 infection in Old World monkeys.** *Nature* 2004, **427**:848-853.
14. Nakayama EE, Miyoshi H, Nagai Y, Shioda T: **A specific region of 37 amino acid residues in the SPRY (B30.2) domain of African green monkey TRIM5alpha determines species-specific restriction of simian immunodeficiency virus SIVmac infection.** *J Virol* 2005, **79**:8870-8877.
15. Hatziioannou T, Perez-Caballero D, Yang A, Cowan S, Bieniasz PD: **Retrovirus resistance factors Ref1 and Lv1 are species-specific variants of TRIM5alpha.** *Proc Natl Acad Sci USA* 2004, **101**:10774-10779.
16. Keckesova Z, Ylinen LM, Towers GJ: **The human and African green monkey TRIM5alpha genes encode Ref1 and Lv1 retroviral restriction factor activities.** *Proc Natl Acad Sci USA* 2004, **101**:10780-10785.
17. Perron MJ, Stremlau M, Song B, Ulm W, Mulligan RC, Sodroski J: **TRIM5alpha mediates the postentry block to N-tropic murine leukemia viruses in human cells.** *Proc Natl Acad Sci USA* 2004, **101**:11827-11832.
18. Reymond A, Meroni G, Fantozzi A, Merla G, Cairo S, Luzi L, Riganelli D, Zanaria E, Messali S, Cainarca S, Guffanti A, Minucci S, Pelicci PG, Ballabio A: **The tripartite motif family identifies cell compartments.** *Embo J* 2001, **20**:2140-2151.
19. Jackson PK, Eldridge AG, Freed E, Furstenthal L, Hsu JY, Kaiser BK, Reimann JD: **The lore of the RINGs: substrate recognition and catalysis by ubiquitin ligases.** *Trends Cell Biol* 2000, **10**:429-439.
20. Anderson JL, Campbell EM, Wu X, Vandegraaff N, Engelman A, Hope TJ: **Proteasome inhibition reveals that a functional preintegration complex intermediate can be generated during restriction by diverse TRIM5 proteins.** *J Virol* 2006, **80**:9754-9760.
21. Wu X, Anderson JL, Campbell EM, Joseph AM, Hope TJ: **Proteasome inhibitors uncouple rhesus TRIM5alpha restriction of HIV-1 reverse transcription and infection.** *Proc Natl Acad Sci USA* 2006, **103**:7465-7470.
22. Maegawa H, Miyamoto T, Sakuragi J, Shioda T, Nakayama EE: **Contribution of RING domain to retrovirus restriction by TRIM5alpha depends on combination of host and virus.** *Virology* 2010, **399**:212-220.
23. Javanbakht H, Diaz-Griffero F, Stremlau M, Si Z, Sodroski J: **The contribution of RING and B-box 2 domains to retroviral restriction mediated by monkey TRIM5alpha.** *J Biol Chem* 2005, **280**:26933-26940.
24. Diaz-Griffero F, Kar A, Perron M, Xiang SH, Javanbakht H, Li X, Sodroski J: **Modulation of retroviral restriction and proteasome inhibitor-resistant**

turnover by changes in the TRIM5alpha B-box 2 domain. *J Virol* 2007, **81**:10362-10378.
25. Kar AK, Diaz-Griffero F, Li Y, Li X, Sodroski J: **Biochemical and biophysical characterization of a chimeric TRIM21-TRIM5alpha protein.** *J Virol* 2008, **82**:11669-11681.
26. Langelier CR, Sandrin V, Eckert DM, Christensen DE, Chandrasekaran V, Alam SL, Aiken C, Olsen JC, Kar AK, Sodroski JG, Sundquist WI: **Biochemical characterization of a recombinant TRIM5alpha protein that restricts human immunodeficiency virus type 1 replication.** *J Virol* 2008, **82**:11682-11694.
27. Li X, Sodroski J: **The TRIM5alpha B-box 2 domain promotes cooperative binding to the retroviral capsid by mediating higher-order self-association.** *J Virol* 2008, **82**:11495-11502.
28. Diaz-Griffero F, Qin XR, Hayashi F, Kigawa T, Finzi A, Sarnak Z, Lienlaf M, Yokoyama S, Sodroski J: **A B-box 2 Surface Patch Important for TRIM5 {alpha} Self-Association, Capsid-binding Avidity and Retrovirus Restriction.** *J Virol* 2009, **83**:10737-51.
29. Mische CC, Javanbakht H, Song B, Diaz-Griffero F, Stremlau M, Strack B, Si Z, Sodroski J: **Retroviral restriction factor TRIM5alpha is a trimer.** *J Virol* 2005, **79**:14446-14450.
30. Javanbakht H, Yuan W, Yeung DF, Song B, Diaz-Griffero F, Li Y, Li X, Stremlau M, Sodroski J: **Characterization of TRIM5alpha trimerization and its contribution to human immunodeficiency virus capsid binding.** *Virology* 2006, **353**:234-246.
31. Nakayama EE, Maegawa H, Shioda T: **A dominant-negative effect of cynomolgus monkey tripartite motif protein TRIM5alpha on anti-simian immunodeficiency virus SIVmac activity of an African green monkey orthologue.** *Virology* 2006, **350**:158-163.
32. Perez-Caballero D, Hatziioannou T, Yang A, Cowan S, Bieniasz PD: **Human tripartite motif 5alpha domains responsible for retrovirus restriction activity and specificity.** *J Virol* 2005, **79**:8969-8978.
33. Sawyer SL, Wu LI, Emerman M, Malik HS: **Positive selection of primate TRIM5alpha identifies a critical species-specific retroviral restriction domain.** *Proc Natl Acad Sci USA* 2005, **102**:2832-2837.
34. Kono K, Song H, Shingai Y, Shioda T, Nakayama EE: **Comparison of anti-viral activity of rhesus monkey and cynomolgus monkey TRIM5alphas against human immunodeficiency virus type 2 infection.** *Virology* 2008, **373**:447-456.
35. Ohkura S, Yap MW, Sheldon T, Stoye JP: **All three variable regions of the TRIM5alpha B30.2 domain can contribute to the specificity of retrovirus restriction.** *J Virol* 2006, **80**:8554-8565.
36. Kono K, Bozek K, Domingues FS, Shioda T, Nakayama EE: **Impact of a single amino acid in the variable region 2 of the Old World monkey TRIM5alpha SPRY (B30.2) domain on anti-human immunodeficiency virus type 2 activity.** *Virology* 2009, **388**:160-168.
37. Perron MJ, Stremlau M, Sodroski J: **Two surface-exposed elements of the B30.2/SPRY domain as potency determinants of N-tropic murine leukemia virus restriction by human TRIM5alpha.** *J Virol* 2006, **80**:5631-5636.
38. Yap MW, Nisole S, Stoye JP: **A single amino acid change in the SPRY domain of human Trim5alpha leads to HIV-1 restriction.** *Curr Biol* 2005, **15**:73-78.
39. Stremlau M, Perron M, Welikala S, Sodroski J: **Species-specific variation in the B30.2(SPRY) domain of TRIM5alpha determines the potency of human immunodeficiency virus restriction.** *J Virol* 2005, **79**:3139-3145.
40. Sebastian S, Luban J: **TRIM5alpha selectively binds a restriction-sensitive retroviral capsid.** *Retrovirology* 2005, **2**:40.
41. Stremlau M, Perron M, Lee M, Li Y, Song B, Javanbakht H, Diaz-Griffero F, Anderson DJ, Sundquist WI, Sodroski J: **Specific recognition and accelerated uncoating of retroviral capsids by the TRIM5alpha restriction factor.** *Proc Natl Acad Sci USA* 2006, **103**:5514-5519.
42. Ylinen LM, Keckesova Z, Wilson SJ, Ranasinghe S, Towers GJ: **Differential restriction of human immunodeficiency virus type 2 and simian immunodeficiency virus SIVmac by TRIM5alpha alleles.** *J Virol* 2005, **79**:11580-11587.
43. Shibata R, Miura T, Hayami M, Ogawa K, Sakai H, Kiyomasu T, Ishimoto A, Adachi A: **Mutational analysis of the human immunodeficiency virus type 2 (HIV-2) genome in relation to HIV-1 and simian immunodeficiency virus SIV (AGM).** *J Virol* 1990, **64**:742-747.
44. Song H, Nakayama EE, Yokoyama M, Sato H, Levy JA, Shioda T: **A single amino acid of the human immunodeficiency virus type 2 capsid affects its replication in the presence of cynomolgus monkey and human TRIM5alphas.** *J Virol* 2007, **81**:7280-7285.
45. Ho SN, Hunt HD, Horton RM, Pullen JK, Pease LR: **Site-directed mutagenesis by overlap extension using the polymerase chain reaction.** *Gene* 1989, **77**:51-59.
46. Gyuris A, Vajda G, Foldes I: **Establishment of an MT4 cell line persistently producing infective HIV-1 particles.** *Acta Microbiol Hung* 1992, **39**:271-279.
47. Kuroishi A, Saito A, Shingai Y, Shioda T, Nomaguchi M, Adachi A, Akari H, Nakayama EE: **Modification of a loop sequence between alpha-helices 6 and 7 of virus capsid (CA) protein in a human immunodeficiency virus type 1 (HIV-1) derivative that has simian immunodeficiency virus (SIVmac239) vif and CA alpha-helices 4 and 5 loop improves replication in cynomolgus monkey cells.** *Retrovirology* 2009, **6**:70.
48. Price AJ, Marzetta F, Lammers M, Ylinen LM, Schaller T, Wilson SJ, Towers GJ, James LC: **Active site remodeling switches HIV specificity of antiretroviral TRIMCyp.** *Nat Struct Mol Biol* 2009, **16**:1036-1042.
49. Gamble TR, Yoo S, Vajdos FF, von Schwedler UK, Worthylake DK, Wang H, McCutcheon JP, Sundquist WI, Hill CP: **Structure of the carboxyl-terminal dimerization domain of the HIV-1 capsid protein.** *Science* 1997, **278**:849-853.
50. Pornillos O, Ganser-Pornillos BK, Kelly BN, Hua Y, Whitby FG, Stout CD, Sundquist WI, Hill CP, Yeager M: **X-ray structures of the hexameric building block of the HIV capsid.** *Cell* 2009, **137**:1282-1292.
51. Deshpande N, Addess KJ, Bluhm WF, Merino-Ott JC, Townsend-Merino W, Zhang Q, Knezevich C, Xie L, Chen L, Feng Z, Green RK, Flippen-Anderson JL, Westbrook J, Berman HM, Bourne PE: **The RCSB Protein Data Bank: a redesigned query system and relational database based on the mmCIF schema.** *Nucleic Acids Res* 2005, **33**:D233-237.
52. Shirakawa K, Takaori-Kondo A, Yokoyama M, Izumi T, Matsui M, Io K, Sato T, Sato H, Uchiyama T: **Phosphorylation of APOBEC3G by protein kinase A regulates its interaction with HIV-1 Vif.** *Nat Struct Mol Biol* 2008, **15**:1184-1191.
53. Labute P: **The generalized Born/volume integral implicit solvent model: estimation of the free energy of hydration using London dispersion instead of atomic surface area.** *J Comput Chem* 2008, **29**:1693-1698.
54. Ponder JW, Case DA: **Force fields for protein simulations.** *Adv Protein Chem* 2003, **66**:27-85.
55. Onufriev A, Bashford D, Case DA: **Modification of the generalized Born model suitable for macromolecules.** *Journal of Physical Chemistry B* 2000, **104**:3712-3720.
56. Onyangoa C, Leligdowicz A, Yokoyamac M, Sato H, Song H, Nakayama EE, Shioda T, Silva T, Townenda J, Jayea A, Whittle H, Rowland-Jones S, Cotten M: **HIV-2 capsids distinguish high and low virus load patients in a West African community cohort.** *Vaccine* 2010, **28S2**:60-67.
57. Braaten D, Franke EK, Luban J: **Cyclophilin A is required for the replication of group M human immunodeficiency virus type 1 (HIV-1) and simian immunodeficiency virus SIV(CPZ)GAB but not group O HIV-1 or other primate immunodeficiency viruses.** *J Virol* 1996, **70**:4220-4227.
58. Besnier C, Takeuchi Y, Towers G: **Restriction of lentivirus in monkeys.** *Proc Natl Acad Sci USA* 2002, **99**:11920-11925.
59. Cowan S, Hatziioannou T, Cunningham T, Muesing MA, Gottlinger HG, Bieniasz PD: **Cellular inhibitors with Fv1-like activity restrict human and simian immunodeficiency virus tropism.** *Proc Natl Acad Sci USA* 2002, **99**:11914-11919.
60. Hatziioannou T, Cowan S, Goff SP, Bieniasz PD, Towers GJ: **Restriction of multiple divergent retroviruses by Lv1 and Ref1.** *EMBO J* 2003, **22**:385-394.
61. Kootstra NA, Munk C, Tonnu N, Landau NR, Verma IM: **Abrogation of postentry restriction of HIV-1-based lentiviral vector transduction in simian cells.** *Proc Natl Acad Sci USA* 2003, **100**:1298-1303.
62. Owens CM, Song B, Perron MJ, Yang PC, Stremlau M, Sodroski J: **Binding and susceptibility to postentry restriction factors in monkey cells are specified by distinct regions of the human immunodeficiency virus type 1 capsid.** *J Virol* 2004, **78**:5423-5437.
63. Lin TY, Emerman M: **Determinants of cyclophilin A-dependent TRIM5 alpha restriction against HIV-1.** *Virology* 2008, **379**:335-341.
64. Hatziioannou T, Princiotta M, Piatak M Jr, Yuan F, Zhang F, Lifson JD, Bieniasz PD: **Generation of simian-tropic HIV-1 by restriction factor evasion.** *Science* 2006, **314**:95.

65. Berthoux L, Sebastian S, Sokolskaja E, Luban J: **Cyclophilin A is required for TRIM5{alpha}-mediated resistance to HIV-1 in Old World monkey cells.** *Proc Natl Acad Sci USA* 2005, **102**:14849-14853.
66. Keckesova Z, Ylinen LM, Towers GJ: **Cyclophilin A renders human immunodeficiency virus type 1 sensitive to Old World monkey but not human TRIM5 alpha antiviral activity.** *J Virol* 2006, **80**:4683-4690.
67. Sokolskaja E, Berthoux L, Luban J: **Cyclophilin A and TRIM5alpha independently regulate human immunodeficiency virus type 1 infectivity in human cells.** *J Virol* 2006, **80**:2855-2862.
68. Stremlau M, Song B, Javanbakht H, Perron M, Sodroski J: **Cyclophilin A: an auxiliary but not necessary cofactor for TRIM5alpha restriction of HIV-1.** *Virology* 2006, **351**:112-120.
69. Khorasanizadeh S, Campos-Olivas R, Clark CA, Summers MF: **Sequence-specific 1H, 13C and 15N chemical shift assignment and secondary structure of the HTLV-I capsid protein.** *Journal of biomolecular NMR* 1999, **14**:199-200.
70. Jin Z, Jin L, Peterson DL, Lawson CL: **Model for lentivirus capsid core assembly based on crystal dimers of EIAV p26.** *J Mol Biol* 1999, **286**:83-93.
71. Mortuza GB, Dodding MP, Goldstone DC, Haire LF, Stoye JP, Taylor IA: **Structure of B-MLV capsid amino-terminal domain reveals key features of viral tropism, gag assembly and core formation.** *J Mol Biol* 2008, **376**:1493-1508.
72. Mortuza GB, Goldstone DC, Pashley C, Haire LF, Palmarini M, Taylor WR, Stoye JP, Taylor IA: **Structure of the capsid amino-terminal domain from the betaretrovirus, Jaagsiekte sheep retrovirus.** *J Mol Biol* 2009, **386**:1179-1192.
73. Kinomoto M, Appiah-Opong R, Brandful JA, Yokoyama M, Nii-Trebi N, Ugly-Kwame E, Sato H, Ofori-Adjei D, Kurata T, Barre-Sinoussi F, Sata T, Tokunaga K: **HIV-1 proteases from drug-naive West African patients are differentially less susceptible to protease inhibitors.** *Clin Infect Dis* 2005, **41**:243-251.
74. Kinomoto M, Yokoyama M, Sato H, Kojima A, Kurata T, Ikuta K, Sata T, Tokunaga K: **Amino acid 36 in the human immunodeficiency virus type 1 gp41 ectodomain controls fusogenic activity: implications for the molecular mechanism of viral escape from a fusion inhibitor.** *J Virol* 2005, **79**:5996-6004.

doi:10.1186/1742-4690-7-72
Cite this article as: Kono *et al.*: Multiple sites in the N-terminal half of simian immunodeficiency virus capsid protein contribute to evasion from rhesus monkey TRIM5α-mediated restriction. *Retrovirology* 2010 **7**:72.

ELSEVIER

Institut Pasteur

Microbes and Infection 15 (2013) 56–65

www.elsevier.com/locate/micinf

Original article

Gag-CA Q110D mutation elicits TRIM5-independent enhancement of HIV-1mt replication in macaque cells

Masako Nomaguchi [a,1], Masaru Yokoyama [b,1], Ken Kono [c], Emi E. Nakayama [c], Tatsuo Shioda [c], Akatsuki Saito [d], Hirofumi Akari [d], Yasuhiro Yasutomi [e], Tetsuro Matano [f], Hironori Sato [b], Akio Adachi [a,*]

[a] *Department of Microbiology, Institute of Health Biosciences, The University of Tokushima Graduate School, 3-18-15 Kuramoto, Tokushima 770-8503, Japan*
[b] *Laboratory of Viral Genomics, Pathogen Genomics Center, National Institute of Infectious Diseases, 4-7-1 Gakuen, Musashimurayama, Tokyo 208-0011, Japan*
[c] *Department of Viral Infections, Research Institute for Microbial Diseases, Osaka University, 3-1 Yamadaoka, Suita, Osaka 565-0871, Japan*
[d] *Center for Human Evolution Modeling Research, Primate Research Institute, Kyoto University, 41-2 Kanrin, Inuyama, Aichi 484-8506, Japan*
[e] *Tsukuba Primate Research Center, National Institute of Biomedical Innovation, Tsukuba, Ibaraki 305-0843, Japan*
[f] *AIDS Research Center, National Institute of Infectious Diseases, 1-23-1 Toyama, Shinjuku-ku, Tokyo 162-8640, Japan*

Received 5 September 2012; accepted 20 October 2012
Available online 1 November 2012

Abstract

HIV-1 is strictly adapted to humans, and cause disease-inducing persistent infection only in humans. We have generated a series of macaque-tropic HIV-1 (HIV-1mt) to establish non-human primate models for basic and clinical studies. HIV-1mt clones available to date grow poorly in macaque cells relative to SIVmac239. In this study, viral adaptive mutation in macaque cells, G114E in capsid (CA) helix 6 of HIV-1mt, that enhances viral replication was identified. Computer-assisted structural analysis predicted that another Q110D mutation in CA helix 6 would also increase viral growth potential. A new proviral construct MN4Rh-3 carrying CA-Q110D exhibited exquisitely enhanced growth property specifically in macaque cells. Susceptibility of MN4Rh-3 to macaque TRIM5α/TRIMCyp proteins was examined by their expression systems. HIV-1mt clones so far constructed already completely evaded TRIMCyp restriction, and further enhancement of TRIMCyp resistance by Q110D was not observed. In addition, Q110D did not contribute to evasion from TRIM5α restriction. However, the single-cycle infectivity of MN4Rh-3 in macaque cells was enhanced relative to the other HIV-1mt clones. Our results here indicate that CA-Q110D accelerates viral growth in macaque cells irrelevant to TRIM5 proteins restriction.

Keywords: HIV-1; HIV-1mt; Gag-CA; Macaque cells; Virus growth; Molecular modeling

1. Introduction

Mammalian cells express a variety of host restriction factors to defend themselves against pathogens. Viruses have evolved countermeasures to subvert their restriction and replicate efficiently in cells [1,2]. HIV-1, a causative agent of human AIDS, evades host restriction factors and replicates well in human cells. However, in macaques for experimental use, e.g. cynomolgus macaques (CyMs) and rhesus macaques (RhMs), HIV-1 replication is completely inhibited by host restriction factors present in their cells [3]. Construction of HIV-1 that overcomes species-barrier contributes much to understand the interaction of HIV-1 and its host as well as the establishment of HIV-1-infected macaque models [4,5].

Extensive molecular biological studies on the HIV-1/host interaction conducted to date have revealed main mechanical bases for the narrow host range exhibited by HIV-1. Macaque cells contain potent antiviral factors that effectively restrict or even abolish HIV-1 replication. These include APOBEC3 proteins (APOs), CyclophilinA (CypA), and TRIM5α/TRIMCyp

* Corresponding author. Tel.: +81 88 633 7078; fax: +81 88 633 7080.
E-mail address: adachi@basic.med.tokushima-u.ac.jp (A. Adachi).
[1] Masako Nomaguchi and Masaru Yokoyama contributed equally to this work.

1286-4579/$ - see front matter © 2012 Institut Pasteur. Published by Elsevier Masson SAS. All rights reserved.
http://dx.doi.org/10.1016/j.micinf.2012.10.013